


## RESEARCH ARTICLE

# Basal forebrain cholinergic neurons are vulnerable in a mouse model of Down syndrome and their molecular fingerprint is rescued by maternal choline supplementation

Melissa J. Alldred<sup>1,2</sup> | Harshitha Pidikiti<sup>1</sup> | Adriana Heguy<sup>3</sup> | Panos Roussos<sup>1,4,5,6</sup> | Stephen D. Ginsberg<sup>1,2,7,8</sup> 

<sup>1</sup>Center for Dementia Research, Nathan Kline Institute, Orangeburg, New York, USA

<sup>2</sup>Department of Psychiatry, New York University Grossman School of Medicine, New York, New York, USA

<sup>3</sup>Genome Technology Center, New York University Grossman School of Medicine, New York, New York, USA

<sup>4</sup>Department of Genetics and Genomic Sciences, Icahn School of Medicine at Mount Sinai, New York, New York, USA

<sup>5</sup>Department of Psychiatry, Icahn School of Medicine at Mount Sinai, New York, New York, USA

<sup>6</sup>The Institute for Data Science and Genomic Technology, Icahn School of Medicine at Mount Sinai, New York, New York, USA

<sup>7</sup>Department of Neuroscience & Physiology, New York University Grossman School of Medicine, New York, New York, USA

<sup>8</sup>NYU Neuroscience Institute, New York University Grossman School of Medicine, New York, New York, USA

## Correspondence

Stephen D. Ginsberg, Center for Dementia Research, Nathan Kline Institute, 140 Old Orangeburg Road, Orangeburg, NY 10962, USA.  
Email: [ginsberg@nki.rfmh.org](mailto:ginsberg@nki.rfmh.org)

## Funding information

HHS | National Institutes of Health (NIH), Grant/Award Number: AG014449, AG017617, AG072599, AG074004 and AG077103

## Abstract

Basal forebrain cholinergic neuron (BFCN) degeneration is a hallmark of Down syndrome (DS) and Alzheimer's disease (AD). Current therapeutics in these disorders have been unsuccessful in slowing disease progression, likely due to poorly understood complex pathological interactions and dysregulated pathways. The Ts65Dn trisomic mouse model recapitulates both cognitive and morphological deficits of DS and AD, including BFCN degeneration and has shown lifelong behavioral changes due to maternal choline supplementation (MCS). To test the impact of MCS on trisomic BFCNs, we performed laser capture microdissection to individually isolate choline acetyltransferase-immunopositive neurons in Ts65Dn and disomic littermates, in conjunction with MCS at the onset of BFCN degeneration. We utilized single population RNA sequencing (RNA-seq) to interrogate transcriptomic changes within medial septal nucleus (MSN) BFCNs. Leveraging multiple bioinformatic analysis programs on differentially expressed genes (DEGs) by genotype and diet, we identified key canonical pathways and altered physiological functions within Ts65Dn MSN BFCNs, which were attenuated by MCS in trisomic offspring, including the cholinergic, glutamatergic and GABAergic pathways. We linked differential gene expression bioinformatically to multiple neurological functions, including motor dysfunction/movement disorder, early onset neurological disease, ataxia and cognitive impairment via Ingenuity Pathway Analysis. DEGs within these identified pathways may underlie aberrant behavior in the DS mice, with MCS attenuating the underlying gene expression changes. We propose MCS ameliorates aberrant BFCN gene expression within the septohippocampal circuit of trisomic mice through normalization of principally the cholinergic, glutamatergic, and GABAergic signaling pathways, resulting in attenuation of underlying neurological disease functions.

## KEYWORDS

Alzheimer's disease, bioinformatics, Down syndrome, laser capture microdissection, maternal choline supplementation, medial septum, RNA-seq, selective vulnerability, trisomy

## 1 | INTRODUCTION

Down syndrome (DS) is a neurodevelopmental and neurodegenerative genetic disorder caused by triplication of human chromosome 21 (HSA21), which is observed in ~1 of 700 births, and is primary cause of intellectual disability.<sup>1,2</sup> DS results in systemic and neurological conditions, including deficits in learning and memory.<sup>3-8</sup> Individuals with DS also display the onset of neurodegeneration associated with Alzheimer's disease (AD) in early mid-life, including amyloid plaques, neurofibrillary tangles, and cognitive decline, with age-associated escalation.<sup>9-16</sup> While persons with DS have significantly improved lifespans due to medical intervention,<sup>17-20</sup> these individuals have increased health complications, with the development of dementia accounting for >70% of deaths in individuals over the age of 35.<sup>21</sup> Age-related cognitive decline in DS and AD is associated with degeneration of the cholinergic basal forebrain system, including neuronal loss in subregions of the basal forebrain and specific loss of cholinergic basal forebrain neurons in the nucleus basalis and cholinergic fiber projections to the hippocampus and neocortex.<sup>4,22-26</sup>

Many human DS neuropathological features are recapitulated in the Ts65Dn mouse model, including basal forebrain cholinergic neuron (BFCN) degeneration, AD-like hippocampal-dependent learning and memory deficits, and septohippocampal circuit degeneration, notably including cholinergic, glutamatergic, and GABAergic dysfunction.<sup>9,27-35</sup> The medial septal nucleus/ventral diagonal band (MSN) of the BFCN system projects to the hippocampus and is critical for learning and memory.<sup>36,37</sup> Degeneration of the BFCN projection system is strongly associated with DS cognitive decline.<sup>30,31,32,38-42</sup> BFCN degeneration is a cardinal feature of the Ts65Dn mouse, beginning at approximately 6 months of age (MO).<sup>29,31,32,40,43-49</sup> BFCN loss and alteration of hippocampal innervation are consistently reported in older (>10 MO) Ts65Dn mice.<sup>32,40,42,50,51</sup> Ts65Dn mice have recently been shown to have significant changes in gene expression within MSN BFCNs at 6 MO by laser capture microdissection (LCM) coupled with single population RNA sequencing (RNA-seq)<sup>52</sup> and in older trisomic mice by LCM coupled with custom-designed microarray analysis.<sup>48</sup> Currently, there is no therapeutic intervention that may slow or stop the BFCN degeneration seen in both mouse and human DS and AD.

Choline is an essential nutrient required for development and homeostasis, and increased consumption of choline is necessary during pregnancy in human and rodent models.<sup>53-55</sup> Choline metabolite plasma levels are depleted in pregnant dams when standard choline levels

are present in rodent chow.<sup>56,57</sup> These reports support the hypothesis that current dietary recommendations for choline are insufficient during pregnancy and lactation.<sup>45,54,55,58</sup> Choline is necessary for proper brain development and function, as it is requisite for biosynthesis of acetylcholine, the primary dietary methyl donor, and is a key substrate in the phosphatidylethanolamine N-methyltransferase (PEMT) pathway. Acetylcholine is a critical neurotransmitter which regulates multiple neurodevelopmental niches including proliferation, migration, and synapse formation, among others,<sup>44,45,59,60</sup> while methylation affects gene expression regulation through epigenetic programming.<sup>61-64</sup> The PEMT pathway utilizes choline as the substrate for formation of several structural membrane phospholipids, including sphingomyelin and phosphatidylcholine.<sup>65,66</sup>

Maternal choline supplementation (MCS) involves increasing dietary choline intake during pregnancy and lactation.<sup>67</sup> MCS is inexpensive and well-tolerated, with numerous publications showing beneficial effects in rodent and human trials.<sup>41,44,55,68-73</sup> MCS positively impacts multiple aspects of learning and memory in offspring of both normal rodents and in disease models.<sup>45,65</sup> MCS has been utilized in the Ts65Dn mouse model with positive behavioral, cellular, and gene expression effects, including benefits in spatial and attentional memory recorded up to 16 MO in Ts65Dn mice, although these effects are not as profound in aged cohorts.<sup>31,41,43,70,74</sup> Further, these trisomic mice have shown morphological benefits in the basal forebrain and hippocampus, along with amelioration of dysfunctional gene expression within hippocampal pyramidal and BFCNs, although these inquiries were limited by the relatively small number of genes queried by microarray analyses.<sup>41,44,48,75,76</sup> Recent human studies have shown long-term clinical benefits of MCS during the 3rd trimester, including improved processing speed in infants and sustained attention in children.<sup>55,77</sup> Understanding the underlying effects of MCS in the adult brain is critical, especially in those with genetic and/or neurodevelopmental abnormalities.

We employed LCM and single population RNA-seq to profile vulnerable BFCNs in the Ts65Dn mouse model of DS in the context of MCS. We postulate by isolating vulnerable MSN BFCNs from heterogenous cell populations and identifying dysregulated genes that are MCS responsive, we will identify targets that underlie the beneficial behavioral and functional changes. Characterizing these select gene and biological pathway targets at the onset of BFCN degeneration will pinpoint the underlying lifelong organizational benefits provided by MCS. These targets may then be utilized for therapeutic intervention that may help slow or stop the progression of BFCN degeneration associated with DS and AD. Further, we hypothesize

differentially expressed genes (DEGs) impacted by MCS could identify previously unknown targets for DS and AD prevention.

## 2 | MATERIALS AND METHODS

### 2.1 | Mice

Animal protocols were approved by the Nathan Kline Institute/New York University Grossman School of Medicine (NYUGSOM) IACUC in accordance with NIH guidelines. Breeder pairs (female Ts65Dn and male C57Bl/6J Eicher × C3H/HeSnJ F1 mice) were purchased from Jackson Laboratories (Bar Harbor, ME, USA) and mated at the Nathan Kline Institute. Breeder pairs were assigned to receive one of two choline-controlled experimental diets: (i) control rodent diet containing 1.1 g/kg choline chloride (AIN-76A; Dyets Inc., Bethlehem, PA), or (ii) choline-supplemented diet containing 5.0 g/kg choline chloride (AIN-76A; Dyets Inc.), as described previously.<sup>31,41</sup> Pups received choline normal or choline supplemented diet as per their respective dam's diet from E0-P21 and starting at weaning (P21) all offspring had ad libitum access to water and the control diet<sup>31,41,42,78,79</sup> (Figure 1A). The choline-supplemented diet provides approximately 4.5 times the concentration of choline in the control diet and is within the normal physiological range.<sup>80</sup> The control diet supplies an adequate level of choline, so the offspring are not choline-deficient, meaning this is not a study of choline deficiency. Tail clips were taken and genotyped<sup>81</sup> at weaning and mice were aged to ~6 MO (Figure 1A).

### 2.2 | Tissue preparation

Brain tissues were accessed from unsupplemented Ts65Dn (Ts;  $n=6$ ), MCS Ts65Dn (Ts+;  $n=8$ ), unsupplemented disomic (2N;  $n=6$ ), and MCS disomic (2N+;  $n=4$ ) male mice (age range: 5.7–6.4 MO, mean age 6.0 MO). Mice were transcardially perfused with ice-cold 0.15 M phosphate buffer as previously described.<sup>76,77,79,80</sup> Brains were immediately flash frozen and 20  $\mu\text{m}$ -thick tissue sections were cryostat cut ( $-25^\circ\text{C}$ ) in the coronal plane (CM1860UV, Leica, Buffalo Grove, IL) and mounted on polyethylene naphthalate (PEN) membrane slides (Leica, Figure 1B). Slides were kept under desiccant at  $-80^\circ\text{C}$  until used for immunohistochemistry. RNase-free precautions were employed, and solutions were made with 18.2 mega Ohm RNase-free water (Nanopure Diamond, Barnstead, Dubuque, IA).

### 2.3 | Immunohistochemistry and neuron collection

PEN membrane slides were equilibrated to room temperature (RT) under desiccant ( $-20^\circ\text{C}$  for 5 min,  $4^\circ\text{C}$  for 10 min, RT for 5 min) followed by a rapid staining protocol utilizing an antibody against choline acetyltransferase (ChAT) (AB144P, Millipore) to preserve intact RNA in the unfixed tissue as previously described (Figure 1B).<sup>52</sup> ChAT-immunoreactive (ir) neurons were identified within the MSN and isolated by LCM (LMD7000; Leica; Figure 1C) as previously described.<sup>52</sup> Approximately 500 ChAT-ir neurons were isolated per brain before proceeding to RNA isolation and RNA-seq library preparation.

### 2.4 | RNA purification

RNA from ~500 BFCNs was purified using miRNeasy Micro kit (Qiagen) according to manufacturers' specifications. A DNase digestion was performed twice sequentially before the final washes and RNA purification. RNA quality control (QC) was performed (RNA 6000 pico kit, Agilent, Santa Clara, CA; Figure 1D).

### 2.5 | Library preparation and RNA-seq

The SMARTer Stranded Total RNA-Seq kit-Pico input Mammalian (Takara Bio, Mountain View, CA) was employed with minor modifications to utilize full volume of RNA.<sup>52</sup> Samples were quantified (Agilent 2100 HS DNA kit; Figure 1D), and samples below 2 nM of library were excluded. Samples were pooled in equimolar concentrations and assayed on an HiSeq-4000 (Illumina, San Diego, CA) using a single read 50 cycle protocol at the NYUGSOM Genome Technology Center (GTC) (Figure 1E,F). Unsupplemented (e.g., normal choline diet) trisomic (Ts) and disomic (2N) RNA-seq profiles were previously generated,<sup>52</sup> utilizing a different bioinformatics interrogation approach and were reanalyzed herein to compare expression profiles with offspring from dams exposed to MCS.

### 2.6 | RNA-seq processing

FastQ files were utilized for all four conditions (2N, 2N+, Ts, Ts+) to analyze data in parallel. FastQ files were generated and QC of the raw reads was performed by FastQC v0.11.9.<sup>82</sup> Read trimming was performed as necessary by Trimmomatic 0.39.<sup>83</sup> If QC passed and showed no adapter contamination, this step was skipped. Sequence

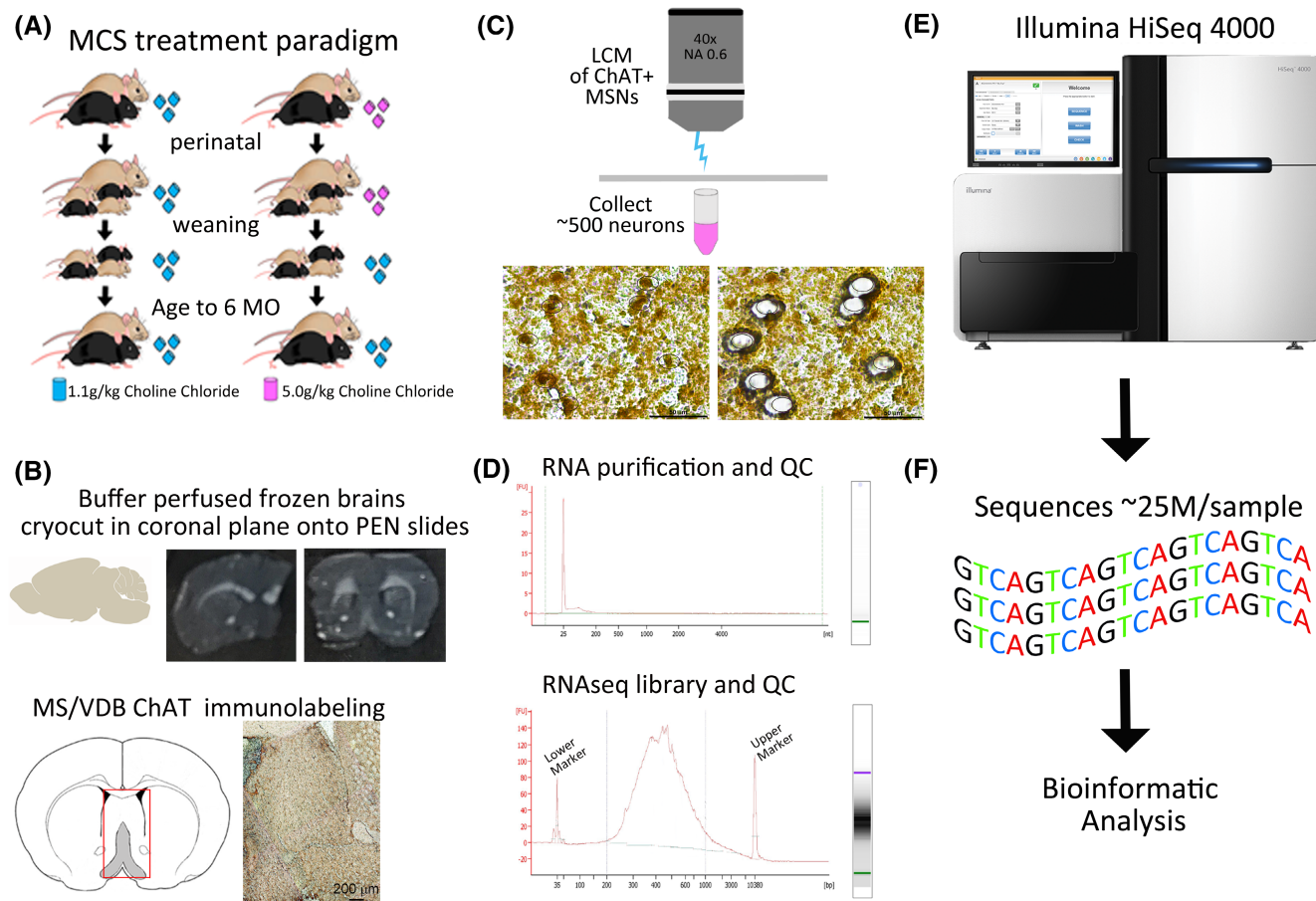


**FIGURE 1** Overview of experimental workflow. (A) The MCS paradigm is shown, with dams and pups fed a normal choline (1.1 g/kg choline) or choline supplemented (+; 5.0 g/kg choline) diet during the perinatal period (E0-P21). Upon weaning (P21), pups are moved to normal choline diet until sacrifice at 6 MO. (B) Brains are immediately flash frozen, cryocut at 20  $\mu$ m, adhered to PEN membrane slides and immunostained for ChAT-ir. (C) LCM is performed on 500 individual MSN BFCNs under a 40X objective. Multiple sections are collected and combined for RNA purification. Scale bar: 50  $\mu$ m. (D) QC is performed on total RNA. RNA-seq library preparation is done, and QC performed on resulting cDNA library for each sample. (E) Illumina HiSeq 4000 single reads were performed by the NYUGSOM GTC. (F) FastQ files were generated for each sample and bioinformatic analysis is initiated.

reads were indexed and aligned to the reference genome (Gencode GRCm39-mm10) using STAR Aligner (2.7.10a).<sup>84</sup> Quantification was performed on aligned reads using Picard (2.27.1)<sup>85</sup> for different measures and RSEM (1.3.3) for output.<sup>86</sup> QC was performed on aligned reads using RSeQC (v4.0.0).<sup>87</sup> Differential gene expression was performed using R version R-v4.2.0/RStudio v1 + 554 using gene expression results with the mouse reference genome (Gencode GRCm39-mm10) (Supporting Information Figure S1 and Figure 2A).

## 2.7 | Statistical analysis

The Gene Count matrix obtained from RSEM was analyzed. Genes with over 0.1 counts per million (CPM) were retained followed by trimmed mean of M-values (TMM) normalization<sup>88</sup> implemented by edgeR<sup>89</sup> for downstream analysis.

This step removes lowly expressed genes as they provide little evidence of differential expression and increase statistical errors and false discovery rates.<sup>90,91</sup> Analyses were performed using the Dream pipeline<sup>92</sup> which is built on top of limma-voom from the VariancePartition<sup>93</sup> package. In addition to Group and RNA concentration, the following variables were included as covariates: Intergenic percentage, Intronic percentage, Uniquely mapped, mRNA base percentage, Usable base percentage, and Correct strand reads percentage. With the exception of Group and RNA concentration, the other covariates are computed from RNA-seq reads by Picard.<sup>86</sup> TopTable (edgeR; v3.38.1) extracts genes that are present for all comparisons.<sup>90</sup> Gene expression differences at ( $p < .05$ ) were considered statistically significant.<sup>90</sup> Protein coding genes were extracted using the R Bioconductor package AnnotationDbi.<sup>94</sup> Multiple testing corrections were performed by false discovery rate (FDR)<sup>95</sup> (Figure 2A).

## 2.8 | Pathway analyses

Pathway analyses consisted of Ingenuity Pathway Analysis (IPA; Qiagen),<sup>96,97</sup> Kyoto Encyclopedia of Genes and Genomes (KEGG),<sup>98</sup> Gene Ontology (GO),<sup>99,100</sup> and STRING<sup>101</sup> in Cytoscape (cutoff 0.4).<sup>102</sup> GO analysis was filtered in excel utilizing key word targets to identify classes of processes affected by genotype and diet. STRING analysis was performed on Ts compared to 2N DEGs. Select genes including cholinergic receptor muscarinic 2 (*Chrm2*), glutamate ionotropic receptor NMDA type subunit 2A (*Grin2a*), and GABA<sub>A</sub> subunit gamma2 (*Gabrg2*) were filtered to isolate direct significant interactions and reanalyzed in STRING for each geneset to determine interactomes dysregulated in Ts mice. Once interactomes were identified, each gene was compared for disease diet effect (Ts+ vs. Ts). This was performed to compare whether genes were still significantly different in the disease state. Genes significantly affected in disease diet drop out of the secondary STRING interactome, with those genes not rescued by diet in disease represented for each interactome.

## 2.9 | Quantitative-real time polymerase chain reaction (qRT-PCR)

Validation was performed by qPCR utilizing the TaqMan Gene Expression Cell to Ct kit (Life Technologies, Grand Island, NY, USA) as described previously.<sup>52</sup> Briefly, ~200 MSN neurons were isolated via LCM based on morphology from adjacent tissue sections in the same animals as utilized for RNA-seq ( $n=6$  per genotype) after Nissl staining {0.1% thionin in sodium acetate (49.44 mM)/acetic acid (3.6 mM) buffer}.<sup>52,103-106</sup> qRT-PCR was performed utilizing 2  $\mu$ L cDNA from 50  $\mu$ L reaction mixture with 22.5  $\mu$ L input RNA. Taqman qPCR primers (Life Technologies) were selected from a subset of DEGs<sup>52</sup> that were significantly MCS responsive as evidenced in multiple pathways (e.g., IPA and KEGG). Probes included calcium/calmodulin-dependent protein kinase II alpha (*Camk2a*; Mm01258148\_m1), *Chrm2* (Mm01167087\_m1), *Grin2a* (Mm00433802\_m1), mitogen-activated protein kinase 8 (*Mapk8*; Mm01218941\_m1), and nerve growth factor receptor (*Ngfr* aka p75<sup>NTR</sup>; Mm01309638\_m1). Samples were assayed in triplicate on a real-time qPCR cycler (PikoReal, ThermoFisher). 2N qPCR products were evaluated from previously published data<sup>52</sup> due to lack of additional sample material. The ddCT method was used to determine relative gene-level differences between groups.<sup>106-108</sup> Glucuronidase Beta (*GusB*; Mm01197698\_m1) qRT-PCR products were utilized as a control, as *GusB* did not show significant changes in RNA-seq data obtained from

BFCNs herein or in previous analyses.<sup>52,104,105</sup> Negative controls consisted of the reaction mixture without input RNA. Sample data was compared with respect to PCR product synthesis for each gene tested. qRT-PCR log-fold changes (LFCs) were utilized in concert with the Cell to Ct protocol as described previously.<sup>52</sup> Violin plots were generated in Graphpad Prism (9.3.1, GraphPad, Boston, MA) normalizing qPCR product synthesis to 2N expression levels.

## 3 | RESULTS

### 3.1 | Effects of MCS on MSN BFCN gene expression at 6 MO

RNA-seq was performed on MSN BFCNs from Ts, Ts+, 2N and 2N+ mice (Figure 1 and Supporting Information Figure S1). RNA-seq reads from BFCNs were mapped, and normalization and covariate analyses were performed using the Dream pipeline<sup>91</sup> (Figure 2A). Variance analysis showed RNA input levels, intronic, and intergenic percentages were covariates and were adjusted accordingly. Principal component analysis (PCA) revealed 2N and 2N+ BFCN profiles cluster closely together while greater variability was observed in Ts and Ts+ BFCN profiles, indicating a stronger genotype and diet effect in Ts mice, with Ts+ profiles showing the most distinct gene expression pattern (Figure 2B). Genotype and diet effects are interrogated by examining DEGs identified by genotype (Ts vs. 2N) and disease diet (Ts+ vs. Ts; Figure 2C). PCA plots and heatmaps of DEGs likely reflect the onset of BFCN degeneration and indicate perinatal MCS has a profound beneficial effect on gene expression within BFCNs. A total of 2510 genes were differentially expressed at  $p < .05$ , with 511 genes reaching significance at FDR  $< .05$ , by genotype (e.g., Ts compared to 2N). The Dream pipeline revealed 138 additional genes at FDR 0.05 and 1067 additional DEGs at  $p < .05$  compared to the limma-voom pipeline (1443 genes<sup>52</sup>), indicating the Dream pipeline enabled us to differentiate small, but significant, differences in gene expression in the current paradigm. Therefore, we demonstrate the Dream pipeline is of high utility when determining DEGs from single population RNA-seq paradigms. Comparing disease diet (e.g., Ts+ vs. Ts), Dream identified 2098 DEGs at  $p < .05$ , with 150 genes reaching significance at FDR  $< 0.05$ . Comparisons for disomic diet (e.g., 2N+ vs. 2N), supplemented genotype (e.g., Ts+ vs. 2N+), and diet plus genotype (Ts+ vs. 2N) revealed fewer DEGs (Figure 3A). Since we are principally examining the effects genotype and diet in the trisomic model, we concentrated our investigation on genotype

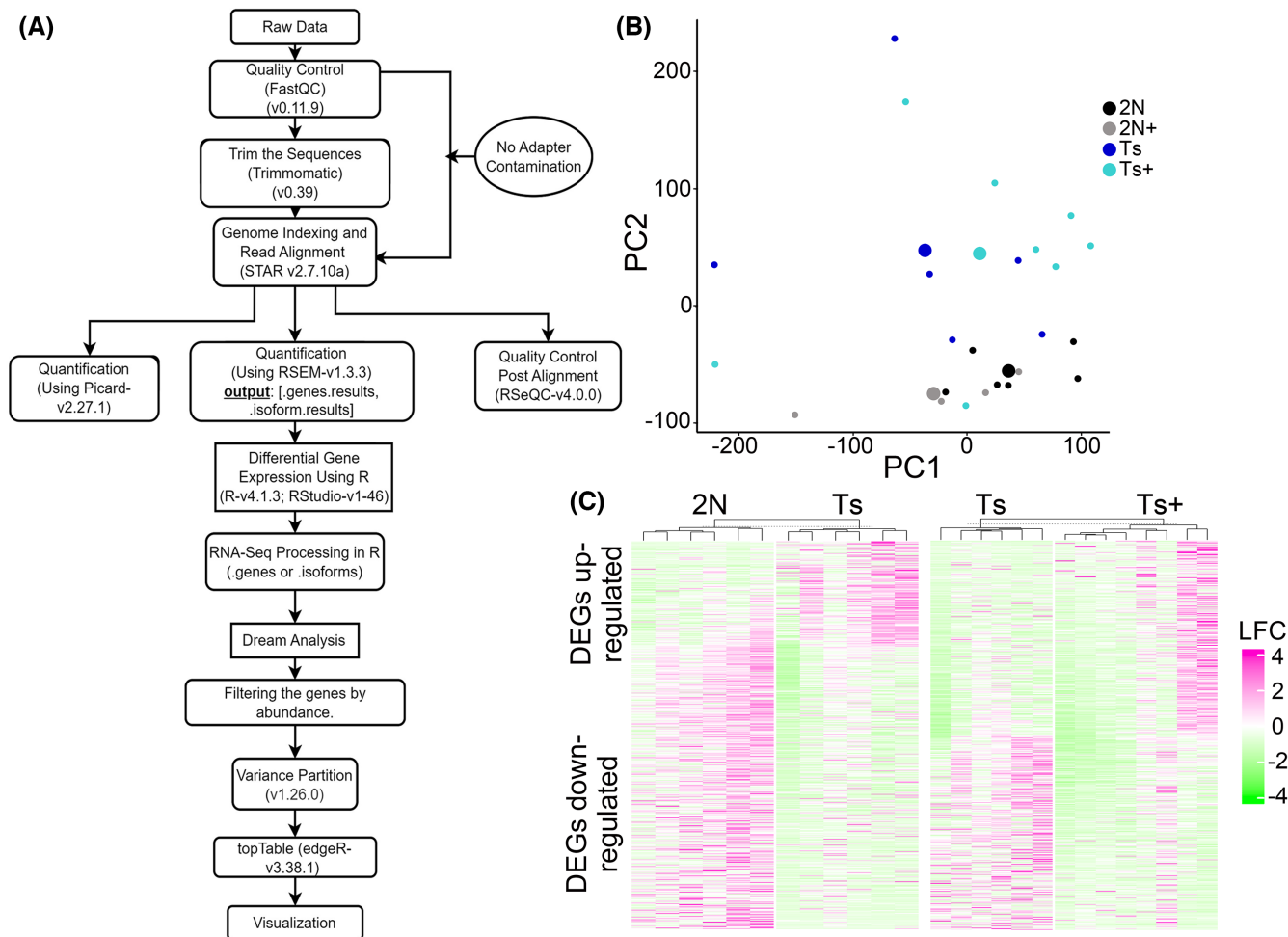


**FIGURE 2** Pipeline for bioinformatic workflow using RNA-seq libraries derived from LCM-captured MSN BFCNs. (A) Workflow for RNA-seq bioinformatics pipeline. (B) PCA shows overall gene expression profiles for each mouse, with mean expression for each group as a larger sized dot. (black = 2N, blue = Ts, gray = 2N+, light blue = Ts+). (C) Heatmaps illustrate individual gene expression differences from each individual mouse with DEGs by genotype (2N and Ts; 2510 DEGs) and disease diet (Ts+ and Ts; 2098 DEGs) binned by upregulation (pink) or downregulation (green).

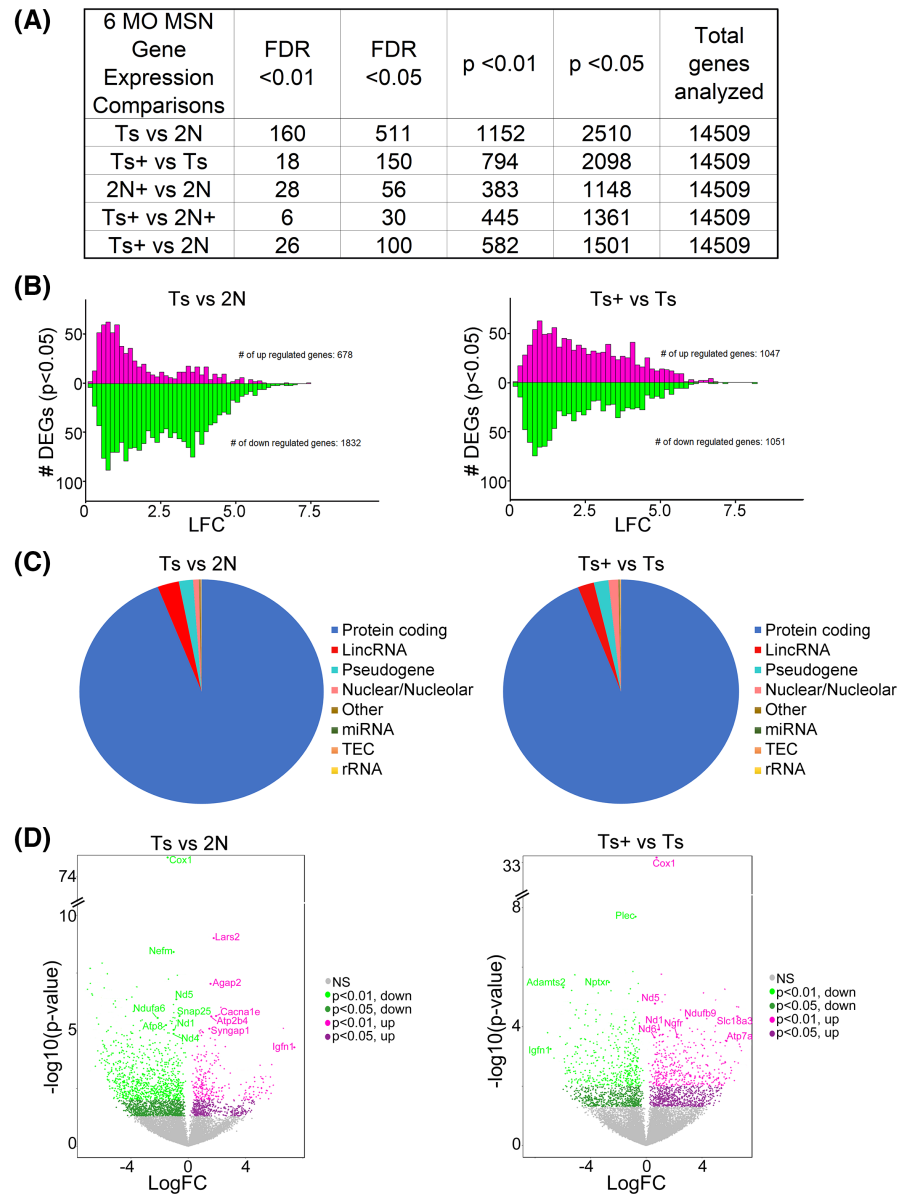
(Ts vs. 2N) and disease diet (Ts+ vs. Ts). The utility of the Dream pipeline is especially evident when querying DEGs by genotype. For example, in trisomic mice ~2.7-fold more downregulated genes were found compared to upregulated genes, with the majority of these DEGs showing small LFCs (<2.5; 57.8%) indicating significant DEGs in trisomic mice, even those with low expression levels, can be readily identified using the Dream pipeline. This observation is confirmed with the disease diet comparison, as Ts+ mice displayed approximately equal numbers of upregulated and downregulated genes, but approximately the same percentage (58.3%) of DEGs with small LFCs (<2.5) compared to genotype (Figure 3B). Over 90% of DEGs were protein coding. The remainder of DEGs were noncoding RNAs (ncRNAs), pseudogenes, and microRNAs (miRNAs) (Figure 3C and Supporting Information Figure S2). Volcano plots demonstrate individual DEGs by diet and genotype via LFC

(Figure 3D and Supporting Information Figure S2C). DEGs for each comparison (genotype × diet) are presented in Supporting Information Tables S1–S5.

### 3.2 | Impact of MCS on triplicated genes

We interrogated triplicated genes dysregulated in BFCNs by genotype and found 14 (of 73 with detectable expression) dysregulated (11 upregulated and 3 downregulated). We queried whether these triplicated genes were impacted in disease diet and found 7 genes significantly rescued in terms of gene expression by MCS. These included DnaJ heat shock protein family (*Hsp40*) member C28 (*Dnajc28*), E26 avian leukemia oncogene 2, 3' domain (*Ets2*), SH3 domain protein 1A intersectin 1 (*Itsn1*), junction adhesion molecule 2 (*Jam2*), MX dynamin-like GTPase 2 (*Mx2*), PAX3 and PAX7 binding protein 1 (*Paxbp1*), and T cell

**FIGURE 3** DEGs are presented by genotype (Ts and 2N) and maternal diet (MCS and normal choline). (A) Table showing the DEGs at each FDR and  $p$ -value cutoff from the total number of analyzed genes. (B) Bar graphs highlighting genes per LFC bin upregulated (pink) and downregulated (green) by genotype and disease diet. (C) Pie charts show percentage of DEGs for protein coding and ncRNAs. (D) Volcano plots show upregulated and downregulated genes with individual genes noted per dot. Light green dots indicate  $p < .01$  downregulated, dark green dots indicate  $p < .05$  downregulated, light pink dots indicate  $p < .01$  upregulated, and dark pink dots indicate  $p < .05$  upregulated.



lymphoma invasion and metastasis 1 (*Tiam1*),  $p < .05$  (Figure 4A) and two trend-level bromodomain and WD repeat domain containing 1 (*Brwd1*) and dual-specificity tyrosine-(Y)-phosphorylation regulated kinase 1a (*Dyrk1a*);  $.05 < p < .1$  (Figure 4B). Only 5 triplicated genes, including DOP1 leucine zipper like protein B (*Dop1b*), receptor-interacting serine-threonine kinase 4 (*Ripk4*), Son DNA binding protein (*Son*), synaptojanin1 (*Synj1*), and tetratricopeptide repeat domain 3 (*Ttc3*) of the 14 genes significantly dysregulated in Ts BFCNs were not MCS responsive in trisomic mice (Figure 4B). Another 4 genes triplicated in Ts65Dn mice that did not show significant genotype differences were disease diet responsive, namely ATP synthase, H<sup>+</sup> transporting, mitochondrial F1 complex, O subunit (*Atp5o*), chaperonin containing Tcp1, subunit 8 (theta) (*Cct8*), potassium inwardly-rectifying channel, subfamily J, member 6 (*Kcnj6*), and solute

carrier family 5 (inositol transporters), member 3 (*Slc5a3*) (Figure 4C). Summating these results, DS triplicated gene expression within BFCNs is significantly decreased in the disease diet (e.g., Ts+ vs. Ts) paradigm (Figure 4B).

### 3.3 | Pathway analysis of DEGs

To determine whether BFCN DEGs linked to biological processes and pathways are selective and/or specific to disease pathogenesis and if MCS ameliorates any of these deficits, we conducted bioinformatic analyses using IPA, KEGG, and GO. By IPA, we found 128 neuronal pathways were dysregulated by genotype (Supporting Information Table S7) and 148 neuronal pathways were impacted in disease diet (Supporting Information Table S8). We queried pathways germane to neurological function

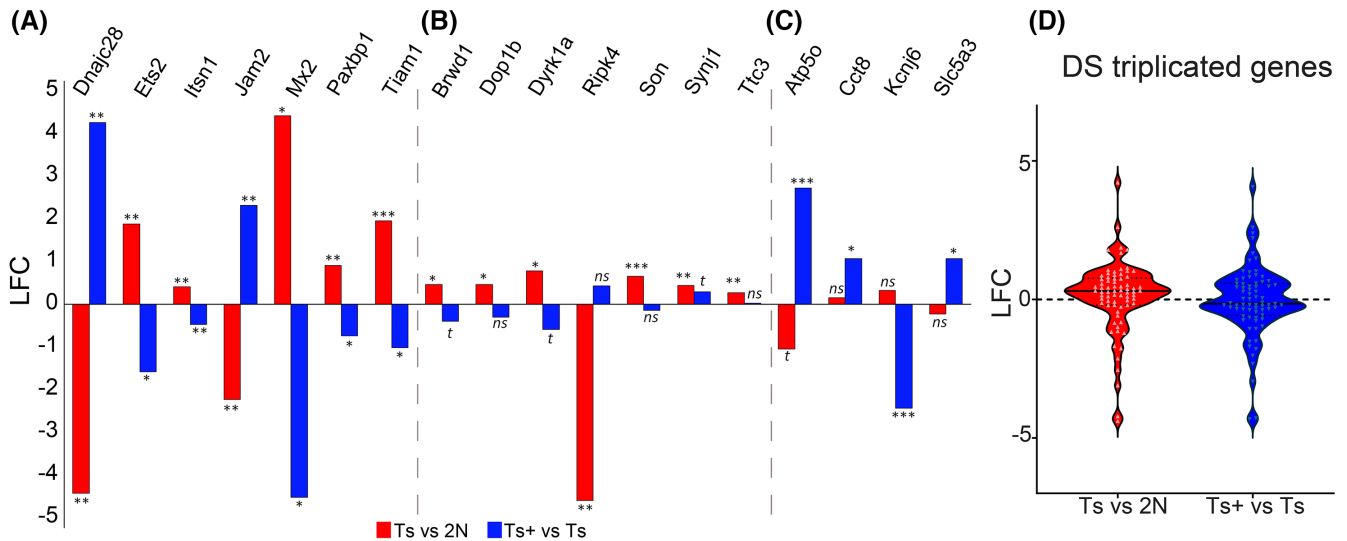


**FIGURE 4** Trisomic protein coding genes do not necessarily match copy number within vulnerable MSN BFCNs. A total of 73 genes (of 88) show quantifiable expression levels with 7 DEGs attaining statistical significance at 6 MO by genotype were rescued in disease diet (A), an additional 7 genes were only affected by genotype (B), and an additional 4 genes were only affected by disease diet (C). Gray vertical dashes delineate DEGs affected by genotype and rescued in disease diet, those significant only by genotype, and those significantly affected by disease diet. (D) Violin plot of 73 triplicated HSA21 orthologs expressed in BFCNs via LFC by genotype and disease diet. Each triangle represents individual gene and LFC amount is represented by thickness of the violin. Key: \*\*\* $p < .001$ , \*\* $p < .01$ , \* $p < .05$ ,  $t = 0.05 > p < .1$ , ns = not significant.

(Figure 5A). MCS effectively reversed dysregulation in several key pathways (seen by z-score) including oxidative phosphorylation, sirtuin signaling, TCA cycle II, synaptic long-term potentiation (LTP), glutamate receptor signaling, superpathway of cholesterol biosynthesis, and synaptic long-term depression (LTD). Not all investigated pathways generated a z-score in IPA to determine directionality (e.g., upregulation and/or downregulation), including mitochondrial dysfunction and GABA receptor signaling (Figure 5A, Supporting Information Tables S7 and S8).

DEGs by genotype and disease diet were also assessed utilizing KEGG. A total of 43 neuronal pathways were identified by genotype and 37 neuronal pathways by disease diet (Supporting Information Tables S9 and S10). Several additional pathways not found by IPA were identified by genotype and disease diet including Thermogenesis, Alzheimer's disease, and Cholinergic Synapse (Figure 5B). Interestingly, the Phosphatidylinositol Signaling System was not altered by genotype, but was significantly affected in disease diet in BFCNs (Figure 5B). We demonstrate DEGs by genotype (red) or disease diet (blue), with a subset of DEGs affected by both genotype and disease diet (purple; Figure 5C,D). DEGs regulated by both genotype and disease diet in specific pathways range from 27% to 86%, with average gene overlap at 41% (genotype) and 45% (disease diet) (Figure 5C). Importantly, of the DEGs that are differentially regulated by both genotype and disease

diet, MCS reverses the genotype effect in >95% of the genes in these pathways (Table 1). We examined pathways where DEGs differ between genotype and disease diet by individual subunit expression within complexes, which can have profound effects on the determination of upregulation or downregulation. This is especially evident in the cholinergic (Figure 5E), glutamatergic (Figure 5F), and GABAergic (Figure 5G) signaling pathways. Within the cholinergic signaling pathway, in addition to downstream effectors that are modulated independently by genotype or disease diet, the choline transporter (*Cht*) and *Chrm2* are rescued by in the Ts+ BFCNs, while the cholinergic receptor muscarinic 1 (*Chrm1*), potassium inwardly rectifying channel subfamily J member 4 (*Kir2.3* aka *Kcnj4*), and potassium inwardly rectifying channel subfamily J member 6 (*Kir3.2* aka *Kcnj6*) receptors, along with the presynaptic *Chat* and vesicular acetylcholine transporter (*VACHT* aka *Slc18a3*) are only significantly changed in disease diet. Conversely, the potassium voltage-gated channel subfamily Q member 5 (*Kv7.5* aka *Kcnq5*) receptor is significantly affected by genotype but not rescued in disease diet (Figure 5E). Within the glutamate receptor signaling pathway, NMDA, AMPA, kainate, and mGluRs are regulated by genotype, disease diet, or both, with a numerous DEGs being genotype and disease diet-dependent or genotype-independent and diet-dependent (Figure 5F). GABAergic receptor signaling shows similar findings, with specific changes in



extrasynaptic subunits regulating tonic inhibition versus synaptic subunits mediating phasic inhibition of the GABA<sub>A</sub> pentameric complex differentially regulated by genotype {synaptic alpha1 (*Gabra1*), alpha3 (*Gabra3*) and extrasynaptic/synaptic beta2 (*Gabrb2*) subunits} and disease diet {extrasynaptic delta subunit (*Gabrd*) or both (synaptic *Gabrg2*)} (Figure 5G).

### 3.4 | Cholinergic, glutamatergic, and GABAergic interactomes modulated by MCS

Analysis by genotype and diet was performed on the 2510 BFCN DEGs which resulted in 2350 proteins identified by STRING in Cytoscape. Interactions were filtered by key receptors or receptor subunits significantly attenuated by MCS. For the cholinergic pathway, a total of 26 DEGs were found in the *Chrm2* interactome (Figure 6A). Of these 26 protein coding genes, 9 were significantly attenuated by disease diet (34.4%), while 18 (66.6%) DEGs were not significantly attenuated (Figure 6B). For the glutamatergic pathway, a total of 67 DEGs were found in the *Grin2a* interactome (Figure 6C). Of these 67 protein coding genes, 25 (37.3%) were significantly attenuated by disease diet (e.g., phenotypic rescue), while 42 (62.7%) DEGs remained significantly dysregulated (Figure 6D). For the GABAergic pathway, a total of 54 DEGs were found in the *Gabrg2* interactome (Figure 6E), in which disease diet rescued 20 (37%) of the DEGs, with 34 (63%) not significantly altered in Ts+ (Figure 6F). When comparing DEGs for supplemented genotype (Ts+ vs. 2N+) and diet plus genotype (Ts+ vs. 2N), we found very few DEGs were still significantly dysregulated in the Ts+ condition within these interactomes, as *Chrm2* had 4 DEGs (15.4%), *Grin2a* had 16 (24.2%) and *Gabrg2* had 16 (29.6%) (Supporting Information Figure S3). Therefore, MCS has a profound effect in rescuing aberrant gene expression within key interactomes in multiple pathways relevant to cognition in trisomic mice.

### 3.5 | MCS effects biological processes beyond pathway analysis

GO analysis examined biological process (BP) dynamics in relation to genotype and disease diet (Table 2). MCS strongly impacted BPs in the categories of RNA modifications, receptor signaling, and synaptic functions (Supporting Information Tables 11 and 12). Examining GO BPs by genotype and disease diet indicated strong modulation by disease diet on dendritic processes (90% overlap), neurotransmitter processes (89% overlap),

and synaptic localization and transport (100% of genotype modulated by disease diet) (Table 2; Supporting Information Tables 11 and 12). In contrast, receptor signaling, activity and localization, and signaling pathways have the most processes that are specifically modified by genotype, with MCS having a more moderate effect (Table 2; Supporting Information Tables 11 and 12).

### 3.6 | MCS benefits memory circuits in trisomic mice

IPA analysis of disease and functions associated with BFCN DEGs revealed several key neurological functions dysregulated in trisomic mice which are rescued by MCS (e.g., disease diet; Figure 7A). Disease diet shows attenuation of dysregulated gene expression within multiple IPA-designated neurological functions, including motor dysfunction or movement disorders, ataxia, cognitive impairment, and early onset neurological disorders (Figure 7B). Significant beneficial effects with disease diet are not found for spatial memory impairment or cell death of cortical neurons disrupted by genotype (Figure 7A). Neurodegeneration is lowered in the disease diet comparison (e.g., Ts+ vs. Ts) but does not reach significance by genotype (e.g., Ts vs. 2N). In the motor dysfunction or movement disorder category, of the >300 curated genes, only 132 have known functional changes, with 30 trisomic DEGs reversed in disease diet and 1 gene showing additive effects (Figure 7C, Table 3). Similarly, in the Ataxia category, of the >75 curated genes, 61 have known functional changes, with 14 trisomic DEGs reversed in disease diet and 2 gene showing additive effects and in the Cognitive impairment category, of the >250 curated genes, 30 have known functional changes, with 7 trisomic DEGs rescued in disease diet (Figure 7C, Table 3). Together, these findings suggest MCS rescues some, but not all, circuits or interactomes involved in memory retention in the Ts+ BFCNs.

### 3.7 | Validation of MCS responsiveness of select DEGs by qRT-PCR

qRT-PCR shows positive correlations with genes validated previously to be dysregulated by genotype. When re-examined in Ts and Ts+ MSN neurons, the Ts versus 2N DEGs correlate to RNA-seq gene expression LFCs ( $R^2 = .8673$ ) (Figure 8A). Moreover, the disease diet comparison revealed an extremely high correlation for MCS-responsive DEGs ( $R^2 = .9363$ , Figure 8A). For example,

*Chrm2* and *Mapk8* were significantly downregulated by genotype (e.g., Ts vs. 2N) using the Dream pipeline and correlate with qPCR results, while these genes were positively upregulated by disease diet (e.g., Ts+ vs. to Ts) MSNs, which also correlate with qRT-PCR results (Figure 8A,B). Similarly, *Grin2a* and *Camk2a* were significantly upregulated by RNA-seq by genotype and significantly downregulated in disease diet, which also correlated with qPCR (Figure 8A,B). Furthermore, *Ngfr* was trend level upregulated by Dream pipeline analysis by genotype ( $p = .08$ ), correlated with qPCR, and was significantly downregulated by disease diet which also correlated with qPCR product synthesis (Figure 8A,B).

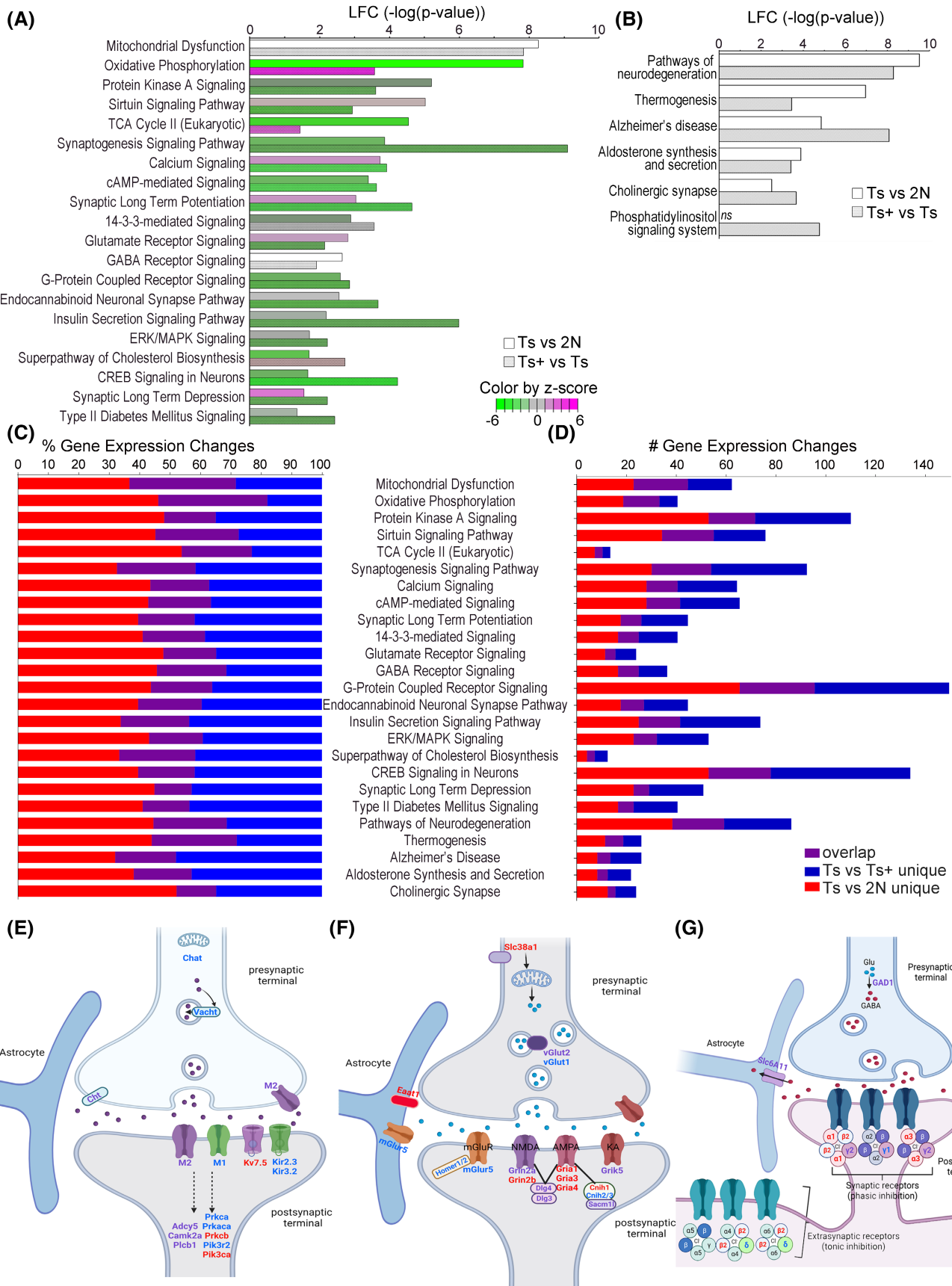
#### 4 | DISCUSSION

Gene expression profiles and pathway analyses were generated using MSN BFCNs in 6 MO mice testing whether early choline delivery beneficially impacted the vulnerable molecular fingerprint of these septohippocampal circuit neurons. Utilizing LCM, we were able to specifically identify and microisolate individual ChAT-ir neurons within the MSN, generating a specific transcriptomic profile of these BFCNs without confounding signals from glial or other neuronal populations. Previous studies showed BFCN degeneration in Ts65Dn mice initiates approximately at 6 MO.<sup>29,38,40,51,109</sup> Relatively few genes from the 'DS critical region' are actually triplicated by expression level in trisomic BFCNs, indicating cell-type specificity for overexpression of triplicated genes. The Dream pipeline identified seven additional significantly upregulated triplicated genes, while three previously identified upregulated triplicated transcripts failed to reach statistical significance (Figure 4A).<sup>52</sup> Interestingly, two DEGs, *Kcnj6* (aka *Kir3.2*) and *Slc5a3*, from the DS critical region which have been identified as disease diet dependent, are involved potassium channel signaling,<sup>110</sup> with *Kcnj6* thought to be expressed and involved at the cholinergic postsynaptic membrane.<sup>111</sup> *Slc5a3* (encoding SMIT1) increases sensitivity of *Kv7.2* and *Kv7.3* potassium channels and is inversely affected by cholinergic M1 receptor firing.<sup>110</sup>

Overall, MCS had a profound beneficial effect on ameliorating triplicated gene expression, including a trend level attenuation of *Dyrk1a*, known to be critically important for normal cognitive development, and altered in DS and AD<sup>112,113</sup> and full reversals of *Dnajc28*, a part of the DnaJ family of heat shock proteins involved in protein folding and molecular chaperones,<sup>114</sup> *Brwd1*, recently shown to be an epigenomic mediator in the Ts mouse model,<sup>115</sup> *Ets2*, an apoptosis pathway mediator,<sup>116</sup> and *Itsn1*, involved in synaptic vesicle recycling.<sup>117</sup> Importantly, rescue of gene expression includes but is not limited to the DS critical region, indicating MCS results in significant modifications within this vulnerable cell type during this key timepoint of cholinergic degeneration onset. We identified numerous DEGs and rescue of aberrant gene expression by MCS (disease diet) to canonical pathways via bioinformatic inquiry and validated several DEGs by qPCR.

Pathway analysis resulted in several key findings for receptor signaling that are MCS responsive in circuits critical for memory and attention. In the cholinergic system several key gene expression level changes are ameliorated in disease diet, including *Chrm2*, which is dysregulated in AD.<sup>118,119</sup> The potassium voltage-gated channels *Kir2.3*, *Kir3.2*, and *Kv7.5* were impacted by genotype and disease diet, which are thought to enable synaptic plasticity at the postsynaptic membrane.<sup>111</sup> Additionally, decreased expression of *VACHT* is modulated in disease diet BFCNs. Loss of VACHT in mouse models and postmortem human AD has been linked to AD pathology, including increased amyloid-beta ( $A\beta$ ) peptides and tau phosphorylation.<sup>120</sup> STRING analysis identified numerous direct interacting partners of *Chrm2* that were dysregulated in trisomic mice and rescued or partially rescued by diet, further indicating that early choline delivery has a profound effect on normalizing the dysregulation seen in cholinergic synaptic activity at the initiation of BFCN degeneration. While current FDA-approved AD therapeutics modulate cholinergic function through inhibiting acetylcholinesterase (AChE), specific targeting of individual receptors for modulation has been difficult.<sup>121</sup> Recently, the cholinergic M1 receptor has been examined for therapeutic intervention in schizophrenia<sup>122</sup> and has shown to be dysregulated at

**FIGURE 5** Bioinformatic assessment of vulnerable pathways in trisomic BFCNs by IPA and KEGG. (A) Bar charts show select pathways identified by IPA dysregulated by genotype and treatment, with LFC represented by each bar (2N vs. Ts white; Ts vs. Ts+ dots), with z-score reflected in coloring (pink upregulated, green downregulated). (B) Pathways uniquely identified by KEGG analysis are shown. (C) Bar graph showing percent gene expression changes within pathways affected by genotype and diet; red = gene changes unique to genotype, purple = gene changes affected by genotype and diet, blue = genes modified by diet in disease. (D) Bar graph shows the number of genes are affected by genotype, diet, or both. (E) Cholinergic pathway is dysregulated by genotype and partially rescued by diet, highlighting specific cholinergic receptor subunits and associated proteins. (F) Glutamate receptor signaling is dysregulated by genotype and partially rescued by disease diet, with NMDA, AMPA, kainite, and metabotropic receptors showing individual subunit gene expression changes. (G) GABA receptor signaling is dysregulated by genotype and modulated by MCS. (C–G, colored red for genotype, blue for MCS, and purple for genes impacted by both genotype and diet).



the protein level in AD.<sup>123</sup> However, the M2 receptor and *VACHT* have not been targeted for therapeutic intervention, although recent evidence is supportive. Specifically,

in a mouse model of AD, chemogenetic-induced increases in *Chrm2* and *VACHT* in the septohippocampal circuit rescued memory impairment.<sup>124</sup>

TABLE 1 Significant IPA canonical pathways identified by DEGs at ( $p < .05$ ).

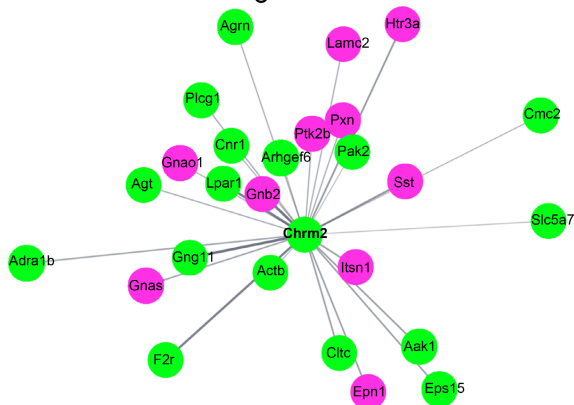
IPA canonical pathway	Modulated by genotype alone	Genotype and disease diet modulated	Modulated in disease diet alone	% Modulated in genotype reversed in disease diet
Mitochondrial dysfunction	22	21	17	100.0
Oxidative phosphorylation	18	14	7	100.0
Protein kinase A signaling	51	18	37	94.4
Sirtuin signaling pathway	33	20	20	90.0
TCA cycle II (Eukaryotic)	7	3	3	100.0
Synaptogenesis signaling pathway	29	23	37	100.0
Calcium signaling	27	12	23	100.0
cAMP-mediated signaling	27	13	23	100.0
Synaptic long term potentiation	17	8	18	100.0
14-3-3-mediated Signaling	16	8	15	100.0
Glutamate receptor signaling	11	4	8	100.0
GABA receptor signaling	16	8	11	100.0
G-protein coupled receptor signaling	40	29	52	86.2
Endocannabinoid neuronal synapse pathway	17	9	17	100.0
Insulin secretion signaling pathway	24	16	31	93.8
ERK/MAPK signaling	22	9	20	100.0
Superpathway of cholesterol biosynthesis	4	3	5	66.7
CREB signaling in neurons	51	24	54	92.0
Synaptic long term depression	22	6	21	100.0
Type II diabetes mellitus signaling	16	6	17	100.0

Dysregulation of glutamate receptor signaling has been shown in DS mouse models, with most studies concentrated on hippocampal dysfunction.<sup>125-127</sup> We show BFCN dysregulation of glutamate receptor signaling is rescued or partially rescued in disease diet. Upregulation of NMDA receptor subunits *Grin2a* and *Grin2b* is found in trisomic mice with *Grin2a* significantly reduced in disease diet, which was corroborated by qRT-PCR, and *Grin2b* partially attenuated. A recent study showed Grin2A protein expression significantly decreases in the absence of choline, which is further exacerbated in an AD mouse model, suggesting this defect is due to alterations of postsynaptic protein concentrations secondary to insufficient choline.<sup>128</sup> Previous studies have shown differential synaptic and peri- or extra-synaptic localization of these subunits, which can be exchanged by lateral

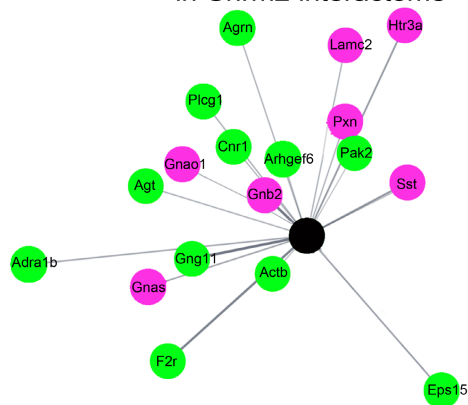
diffusion to finely modulate synaptic strength.<sup>129</sup> Perhaps even more intriguing, ratio imbalances between *Grin2a* and *Grin2b* increased cognitive decline and activation of *Grin2b* containing receptors has been linked to AD due to glutamate excitotoxicity.<sup>130</sup> AMPA receptor subunits also show differential expression in trisomic mice for glutamate ionotropic receptor AMPA type subunits (*Gria1*, *Gria3*, and *Gria4*) that are essentially not MCS responsive, indicating differential effects of MCS on select NMDA and AMPA subunits, which may partially explain the amelioration of some but not all memory circuits by this dietary intervention. However, MCS does significantly decrease *Gria2* expression independent of genotype, which may be relevant to AD pathobiology as postmortem human hippocampal neuron studies indicate upregulation of *Gria2* in AD and pre-pathology ApoE4 carriers.<sup>131,132</sup> Moreover,

FIGURE 6 STRING analysis of select DEGs in Cytoscape. (A) Chrm2 was selected from the Cholinergic pathway to identify genotype DEGs within the interactome, with 26 DEGs directly linked the Chmr2 interactome. (B) A total of 9 trisomic interactome genes are significantly modulated with 18 DEGs within the interactome not significantly modulated in disease diet. (C) Grin2A was selected from the glutamatergic neurotransmission pathway to identify genotype DEGs within the interactome. (D) A total of 25 trisomic interactome genes are significantly rescued by disease diet and 42 (of 67) genes were not significantly attenuated by disease diet in the Grin2A glutamatergic interactome. (E) From the GABAergic pathway, the Gabrg2 interactome contains 54 DEGs. (F) A total of 20 trisomic interactome genes are rescued by MCS in Ts BFCNs and 34 of the DEGs within the Gabrg2 interactome are not significantly attenuated following MCS exposure. Key: pink DEGs, upregulated; green DEGs, downregulated.

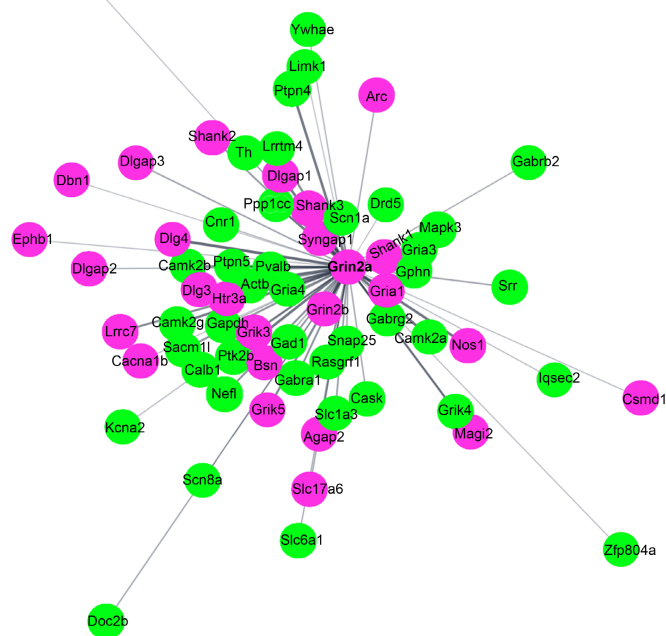
**(A)** DEGs by Genotype in Cholinergic Chrm2 interactome



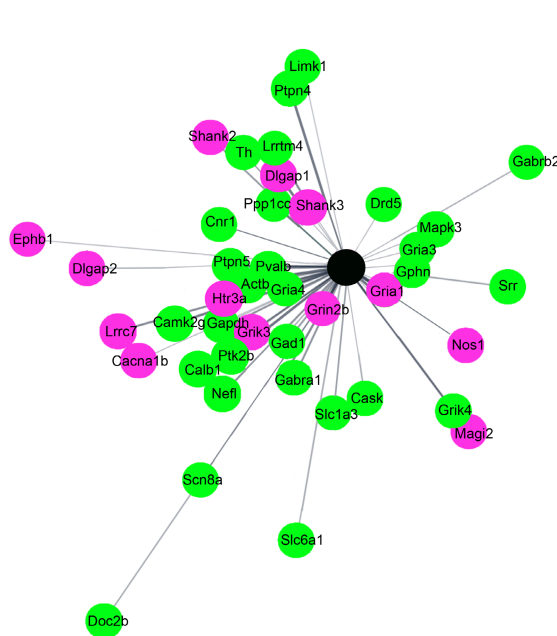
**(B)** MCS Independent DEGs in Chrm2 interactome



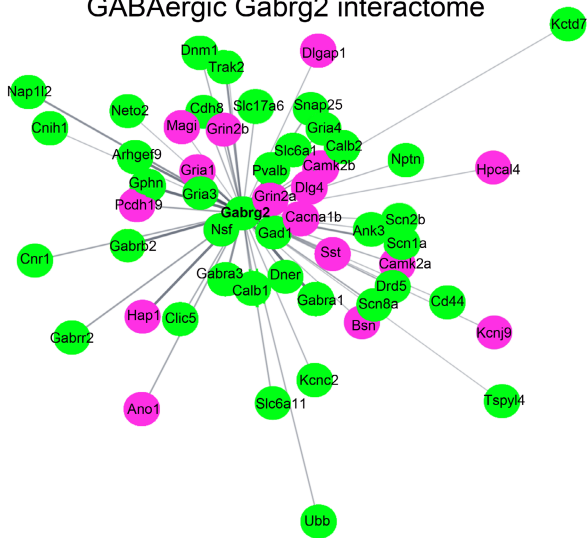
**(C)** DEGs by Genotype in Glutamatergic Grin2a interactome



**(D)** MCS Independent DEGs in Grin2a interactome



**(E)** DEGs by Genotype in GABAergic Gabrg2 interactome



**(F)** MCS Independent DEGs in Gabrg2 interactome

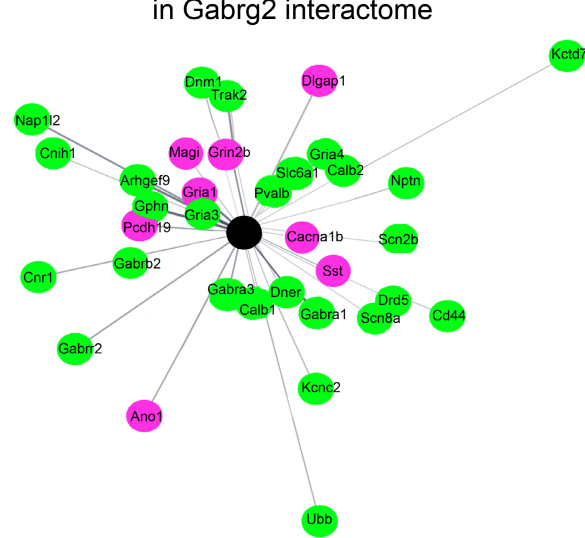


TABLE 2 Significant biological processes linked to DEGs ( $p < .05$ ) in GO filtered by keywords.

Filter term	Ts versus 2N unique processes regulated	Ts versus 2N overlapping processes regulated	Ts+ versus Ts unique processes regulated	Ts+ versus Ts overlapping processes regulated
RNA	15 (44%)	19 (56%)	29 (60%)	19 (40%)
Protein posttranslational modifications	12 (36%)	21 (64%)	17 (45%)	21 (55%)
Protein localization and transport	24 (46%)	28 (54%)	16 (36%)	28 (64%)
Signaling pathways	23 (49%)	24 (51%)	33 (58%)	24 (42%)
Signal transduction	7 (41%)	10 (59%)	7 (41%)	10 (59%)
Receptor signaling, activity and localization	15 (38%)	25 (63%)	37 (60%)	25 (40%)
Dendritic processes	10 (53%)	9 (47%)	1 (10%)	9 (90%)
Axonal processes	4 (21%)	15 (79%)	4 (21%)	15 (79%)
Endo- and exocytosis processes	5 (29%)	12 (71%)	5 (29%)	12 (71%)
Neurodevelopmental processes	8 (26%)	23 (74%)	7 (23%)	23 (77%)
Neurotransmitter processes	15 (65%)	8 (35%)	1 (11%)	8 (89%)
Synaptic transmission and function	10 (34%)	19 (66%)	20 (51%)	19 (49%)
Synaptic vesicle processes	19 (54%)	16 (46%)	5 (24%)	16 (76%)
Synaptic localization and transport	0 (0%)	10 (100%)	11 (52%)	10 (48%)

gene expression for discs large MAGUK scaffold protein 4 (*Dlg4* encoding PSD-95) and discs large MAGUK scaffold protein 3 (*Dlg3* encoding SAP-102) were upregulated in trisomic BFCNs and significantly decreased in disease diet. Both of these postsynaptic binding proteins have been implicated in NMDA and AMPA synaptic scaffolding, trafficking, and re-localizing for internalization.<sup>133</sup> Additionally, attenuation of aberrant gene expression was seen in a multitude of glutamatergic scaffolding proteins (Figure 6C), including *Shank1/2/3*, *Dlgap3*, and *Sacm1l*.<sup>134</sup> The glutamate metabotropic receptor 5 (*Grm5*) is upregulated in trisomic BFCNs and downregulated by MCS (Figure 5F), paralleling observations of increased *Grm5* in individuals with DS.<sup>135</sup> This finding may have translational implications as reduction in GRM5 protein levels induces normal protein synthesis and re-establishes correct levels of LTD, ameliorating learning deficits in a Fragile X mouse model.<sup>136</sup> Taken together, these data suggest MCS has a beneficial effect on glutamatergic transmission. We postulate that early choline delivery may exert these effects by protecting against excitotoxicity and rebalancing overall glutamatergic signaling during the onset of BFCN degeneration.

GABA-mediated over inhibition has also been observed in DS, in mouse models, and postmortem human brain<sup>137-139</sup> with modulation of GABA receptor subunits proposed for clinical treatment of DS.<sup>140</sup> We demonstrate the GABA receptor signaling pathway is vulnerable in trisomic mice and impacted by maternal diet in BFCNs. Previous work has shown choline in the diet is critical for GABAergic transmission with choline supplementation

increasing the density of benzodiazepine receptor sites, with a mechanism of action likely involving membrane phospholipids.<sup>141</sup> Importantly, we found MCS is beneficial for select GABA<sub>A</sub> receptor subunits dysregulated in the context of DS. Either full or partial rescue was found for several key GABA<sub>A</sub> receptor subunits, specifically those known to affect subcellular localization and function. The gamma 2 subunit is critical for postsynaptic localization of GABA<sub>A</sub> receptors<sup>142,143</sup> and was significantly downregulated in trisomic BFCNs and significantly upregulated by MCS, suggesting higher concentrations of synaptic GABA<sub>A</sub> receptors. The postsynaptic clustering protein gephyrin (*Gphn*) was also partially rescued in trisomic BFCNs by MCS. *Gphn* is the main scaffolding protein at GABAergic postsynaptic sites.<sup>144</sup> Concomitantly, a significant decrease in the GABA<sub>A</sub> delta subunit was seen in the disease diet comparison. GABA<sub>A</sub> delta subunits are localized to extrasynaptic clusters, mediating tonic inhibition.<sup>137,145</sup> These concurrent changes likely have a significant beneficial effect on the input-output relationship within these vulnerable BFCNs, essentially increasing the ability of the GABA<sub>A</sub> receptors to facilitate an action potential threshold of synchronized inputs (phasic inhibition) and decreasing the tonic inhibition, which reduces the magnitude duration and propagation of excitatory post-synaptic potentials.<sup>35</sup>

A comprehensive strategy for treatment of cognitive decline in DS through targeting multiple neurotransmitter systems has been proposed.<sup>146</sup> In support of this moderating multiple transmitter systems approach, we show MCS modulates BFCN gene expression not only for specific transcripts but beneficially impacts cholinergic,

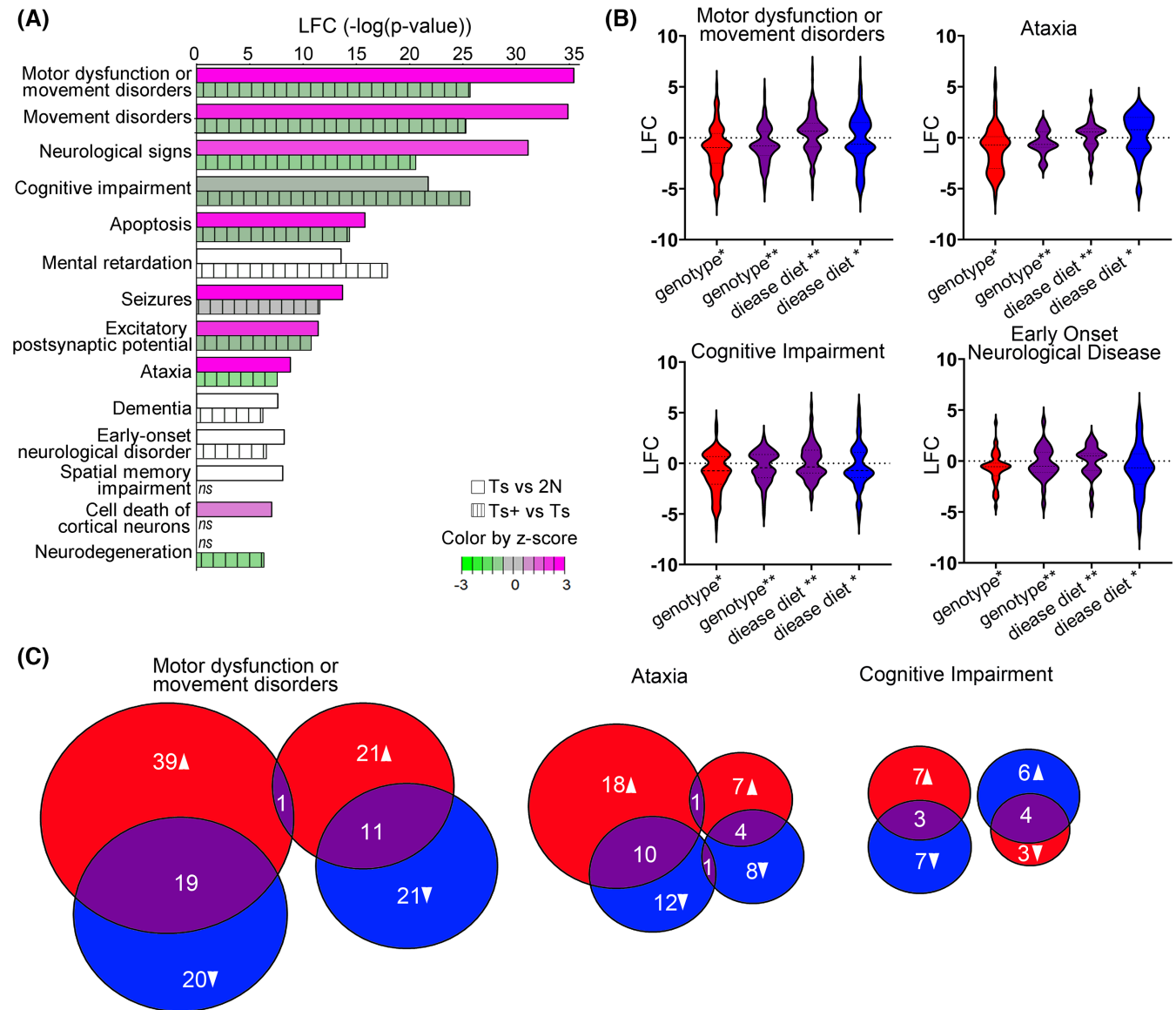


**FIGURE 7** DEGs by genotype and diet were interrogated in IPA for disease and functional correlations. (A) Bar chart identifies key disease and behavioral functions that have underlying molecular changes due to genotype (no pattern) or disease diet (striped pattern). Z-scores of changes for genotype and disease diet are colored with green indicating downregulation and pink representing upregulation. (B) Violin plots show LFC of DEGs unique to genotype (\* red), genotype changes that overlap with disease diet (genotype\*\* purple), disease diet that overlap with genotype (disease diet\*\* purple), and unique to disease diet (\* blue) in four representative pathways of neurological function. (C) Venn diagrams illustrate within motor dysfunction and movement disorders, cognitive impairment, and ataxia neurological functions for DEGs upregulated or downregulated (up arrow or down arrow) by disease in genotype (red) which are modulated by MCS (purple) and those that are only MCS responsive (blue).

glutamatergic, and GABAergic pathways. Specifically, we identified and examined three potential receptor-mediated targets for intervention within these pathways, *Chrm2*, *Grin2a*, and *Gabrg2*. These key targets are modulated by MCS and may also reflect the central moderators of an excitatory/inhibitory (E/I) ratio imbalance that has been postulated to underlie BFCN degeneration and has been found in Ts65Dn mice within multiple brain regions.<sup>27,28,147,148</sup> We postulate that MCS, previously shown to modulate the PEMT pathway and increase

phosphocholine metabolites,<sup>66</sup> normalizes expression of these phospholipids in trisomic BFCNs, and may stabilize the postsynaptic membrane for proper synaptic function and expression of both excitatory and inhibitory receptors. We show MCS beneficially impacts these multiple synaptic and neurotransmitter pathways. Notably, multiple markers of synaptic LTP and LTD are normalized in the disease diet comparison, suggesting MCS rebalances the E/I ratio within trisomic BFCNs, which in turn may protect the septohippocampal circuit.

TABLE 3 DEGs in select disease and functions (IPA) that were modulated by MCS.

Select disease and functions significantly changed in disease and diet	<i>p</i> -value Ts versus 2N	Activation <i>z</i> -score: Ts versus 2N	# Molecules Ts versus 2N	<i>p</i> -value Ts+ versus Ts	Activation <i>z</i> -score Ts+ versus Ts	# Molecules Ts+ versus Ts
Abnormal morphology of neurons	2.54E-18		155	3.84E-14		127
Abnormality of cerebral cortex	1.2E-07	1.663	66	1.92E-07	-1.39	58
Apoptosis of neurons	1.89E-10	2.561	116	2.91E-07	0.908	92
Ataxia	1.56E-09	2.921	85	2.65E-08	-1.568	72
Cellular homeostasis	9.65E-09	-3.875	370	6.7E-12	1.552	336
Cognitive impairment	1.88E-22	-0.232	263	2.28E-26	-0.758	243
Congenital neurological disorder	5.3E-13	0.928	219	1.13E-15	-0.447	201
Dementia	2.42E-08		158	5.82E-07		132
Disorder of basal ganglia	5.81E-31	1.165	283	3.58E-19	-0.482	219
Dominant mental retardation	1.38E-09		51	7.64E-16		57
Dyskinesia	6.88E-26		230	6.95E-18		183
Early-onset neurological disorder	5.86E-09		75	2.86E-07		62
Epilepsy or neurodevelopmental disorder	2.01E-16	1.212	208	4.38E-20	0.377	194
Excitatory postsynaptic potential	3.76E-12	2.268	52	1.72E-11	-0.793	46
Exocytosis	9.86E-08	-1.133	53	1.31E-07	0.268	47
Familial mental retardation	6.73E-12		115	2.03E-15		111
Long-term potentiation	2.64E-15	-0.055	87	1.11E-14	-1.031	77
Mental retardation	2.79E-14		183	1.21E-18		174
Morphogenesis of neurons	2.38E-25	-0.009	204	7.4E-30	-2.774	192
Motor dysfunction or movement disorder	3.82E-36	2.91	390	2.14E-26	-0.849	317
Movement Disorders	1.39E-35	2.53	385	5.18E-26	-0.869	313
Neurodevelopmental disorder	4.31E-15		139	1.69E-16		127
Neurological signs	7.58E-32	1.727	275	2.71E-21	-1.083	217
Neuronal cell death	3.33E-15	1.273	202	1.42E-12	0.693	169
Neurotransmission	7.25E-21	0.603	138	4.96E-21	-0.936	124
Plasticity of synapse	1.64E-12	-0.767	50	3.03E-12	-0.58	45
Potentiation of synapse	1.49E-15	-0.121	88	1.81E-15	-0.885	79
Seizures	1.98E-14	3.084	147	2.68E-12	0.038	124
Synaptic depression	2.42E-09	-0.292	46	2.01E-12	-0.882	47
Synaptic transmission	8.89E-18	1.2	112	1.6E-21	-1.362	108
Cell death of cerebral cortex cells	6.36E-08	1.738	62	ns		
Size of cells	1.06E-07		135	ns		
Action potential of neurons	1.99E-08	-0.636	43	ns		
Excitatory postsynaptic potential of neurons	1.63E-10		28	ns		
Endocytosis	3.41E-09	-3.104	140	ns		
Memory deficits	6.08E-08	0.88	37	ns		
Progressive neurological disorder	6.98E-10	1.219	263	ns		
Spatial memory impairment	7.99E-09		28	ns		
Alzheimer disease or frontotemporal dementia	3.59E-07		140	ns		
Degenerative dementia	3.12E-07		141	ns		



TABLE 3 (Continued)

Select disease and functions significantly changed in disease and diet	p-value Ts versus 2N	Activation z-score: Ts versus 2N	# Molecules Ts versus 2N	p-value Ts+ versus Ts	Activation z-score Ts+ versus Ts	# Molecules Ts+ versus Ts
Tauopathy	2.67E-07		146	ns		
Autophagy	ns			1.23E-07	1.005	122
Cell viability of nervous tissue cell lines	ns			6.3E-08	2.773	30
Long-term synaptic depression of neurons	ns			1.38E-07	-1.917	27
Long-term potentiation of hippocampus	ns			8.1E-09	0.403	35
Miniature excitatory postsynaptic currents	ns			2.04E-07		21
Neurodegeneration	ns			4.69E-07	-1.338	72
Polarity of cells	ns			1.54E-07	-1.036	23
Size of neurons	ns			1.34E-07		30
Transport of vesicles	ns			1.52E-07	0.209	35

Abbreviation: ns, not significant.

GO analysis identified key biological processes involved in neurodevelopment, synaptic localization and transport, protein post-translational modification and receptor signaling, activity and localization. IPA analysis identified neurological disease and function changes including motor dysfunction and memory deficits, cognitive impairment and ataxia all of which showed lifelong (e.g., up to 6 MO) modulation by MCS. These disease and functions are also implicated the *Chrm2*, *Grin2a*, and *Gabrg2* subunits and their interactomes (Figs, 6, 7). Therefore, benefits conferred by MCS may underlie well-established spatial and attentional behaviors seen in Ts65Dn offspring.<sup>41,43,46,59,67,75</sup> Aggregating pathway findings mechanistically, these data suggest MCS provides organizational changes that positively benefit attention, spatial memory, and both short and long-term recognition memory improvements in this DS mouse model which has been corroborated through previous behavioral studies by our collaborative group.<sup>41,42,43,46,70</sup> By identifying and targeting select gene expression and pathway changes, we may isolate novel targets for therapeutic intervention and modulation for translation to DS and possibly AD.

While we strive to eliminate extraneous variables in the data, there remain limitations that may affect outcomes. These include variability in RNA quality, although differences due to genotype are unlikely<sup>75,76,78,79</sup> and RNA quantity was normalized during bioinformatic analysis. It is possible that choline supplementation may also have unintended negative effects on developing pups or on gene expression within the brain, although we find this unlikely as multiple studies from our lab and other independent groups demonstrated the benefits of MCS using a variety of paradigms including RNA-seq, qRT-PCR, immunocytochemistry, and behavioral testing.<sup>45,59,62,67,75,76</sup>

Additionally, choline is a water soluble, essential nutrient, meaning it is unlikely to lead to toxic levels within the body.<sup>45,67,149</sup> We limited this study to male mice, and there may exist sex differences in BFCN degenerative programs.<sup>30</sup> BFCN transcriptomic analyses in female trisomic mice are in progress. However, mixed sex studies have not previously revealed significant differences in gene expression or MCS effects within hippocampal CA1 pyramidal neuron studies.<sup>75,76,78</sup> In terms of IPA analysis of canonical pathways and neurological disease and memory circuit changes, not all of the DEGs identified can be classified as upregulated or downregulated, due to a lack of, or confounding evidence, in the literature.<sup>150</sup> However, we found BFCN gene expression level changes showed a direct correlation between the degenerating septohippocampal circuit and behavioral perturbations in the same trisomic animal model.<sup>41,42,45,46,74</sup> While we utilized the Ts65Dn mouse model, as previously done in MCS behavioral studies,<sup>41,42,43,45,70</sup> several additional DS mouse models exist that may reflect differences in gene expression or effects of MCS, as they vary in the numbers of triplicated HSA21 orthologs.<sup>151-155</sup> We will consider evaluating MCS in the context of septohippocampal circuit neuroprotection utilizing alternative models of DS and AD pathobiology as part of future studies.

Future assessments will also include comparing gene and pathway changes due to MCS on the entire septohippocampal connectome, including GABAergic projection neurons within the MSN that project to hippocampus<sup>155,156</sup> and CA1 hippocampal neurons in the same animals. Interrogation of astrocyte, oligodendrocyte, and microglial populations is beyond the scope of this work, but may show significant effects, as seen in an AD mouse model following early choline delivery.<sup>74</sup>

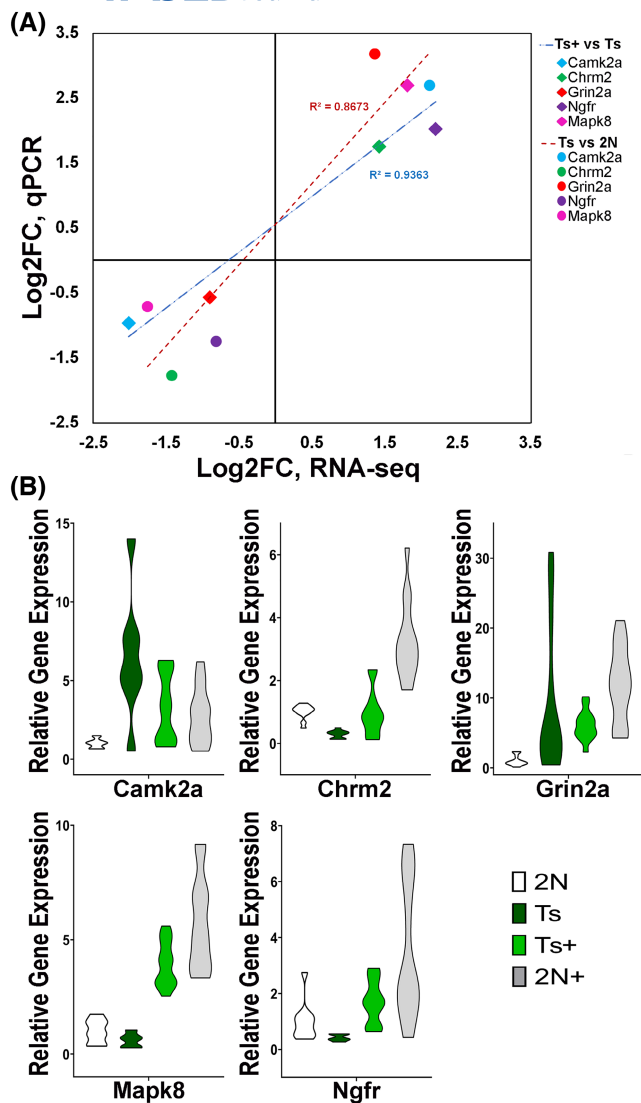


**FIGURE 8** Select DEGs by genotype and diet were validated by qRT-PCR. (A) LFC of the means for qPCR synthesis products were correlated with RNA-seq gene expression data for genotype (circles) and disease diet (diamonds). Trend lines were generated to show correlation between qRT-PCR and RNA-seq LFCs. Key: red dashes, genotype; blue dot/dash, disease diet. (B) Violin plots show relative gene expression levels for the interrogated genes. *Camk2a*, *Chrm2*, *Grin2a*, and *Mapk8* are significantly dysregulated via RNA-seq by genotype and significantly attenuated by MCS in Ts+ MSN BFCNs. *Ngfr* was trend level dysregulated via RNA-seq by genotype and significantly attenuated by MCS. qRT-PCR validated the directionality of all these DEGs found by RNA-seq. Key: 2N, white; Ts, dark green; Ts+, light green; 2N+, gray.

## 5 | CONCLUSIONS

Through single population RNA-seq we have gene and pathway evidence for concomitant cholinergic, glutamatergic, and GABAergic dysfunction within trisomic MSN BFCNs at the onset of degeneration. We demonstrate dysregulation of a complex interconnected

signaling relationship between cholinergic, glutamatergic, and GABAergic signaling that is rescued or partially rescued by MCS in trisomic mice. We also identify novel gene expression changes within vulnerable BFCNs that could be used for therapeutic intervention and modulation for DS and AD pathology within the septohippocampal circuit that may have organizational neuroprotective effects on the brain in both neurodevelopmental and neurodegenerative contexts.

## AUTHOR CONTRIBUTIONS

Melissa J. Alldred, Panos Roussos, and Stephen D. Ginsberg designed experiments. Melissa J. Alldred and Harshitha Pidikiti performed experiments. Melissa J. Alldred, Harshitha Pidikiti, Adriana Heguy, Panos Roussos, and Stephen D. Ginsberg performed statistical analysis. Melissa J. Alldred and Stephen D. Ginsberg wrote manuscript. All authors read and approved final manuscript.

## ACKNOWLEDGMENTS

We thank Arthur Saltzman, M.S., Gabriel E. Hoffman Ph.D., Amanda Labuza, Ph.D., and Paul Zappile, M.S. for expert technical assistance.

## FUNDING INFORMATION

Funding was provided by support from grants AG014449, AG017617, AG072599, AG074004, and AG077103 from the National Institutes of Health.

## DISCLOSURES

The authors reported no biomedical financial interests or potential conflicts of interest.

## DATA AVAILABILITY STATEMENT

Included in article: The data that support the findings of this study are available in the Methods and/or Supplementary Material of this article. Any additional study data study are available on request from the corresponding author. RNA-seq data analyzed within this study are available from the corresponding author upon request.

## ETHICS STATEMENT

Animal protocols were approved by the Nathan Kline Institute/NYUGSOM IACUC in accordance with NIH guidelines.

## ORCID

Stephen D. Ginsberg  <https://orcid.org/0000-0002-1797-4288>

## REFERENCES

1. Parker SE, Mai CT, Canfield MA, et al. Updated National Birth Prevalence estimates for selected birth defects in the

- United States, 2004–2006. *Birth Defects Res A Clin Mol Teratol.* 2010;88:1008-1016.
2. Mai CT, Isenburg JL, Canfield MA, et al. National population-based estimates for major birth defects, 2010–2014. *Birth Defects Res.* 2019;111:1420-1435.
  3. Mann DM, Yates PO, Marcyniuk B. Alzheimer's presenile dementia, senile dementia of Alzheimer type and Down's syndrome in middle age form an age related continuum of pathological changes. *Neuropathol Appl Neurobiol.* 1984;10:185-207.
  4. Coyle JT, ML, Reeves RH, Gearhart JD. Down syndrome, Alzheimer's disease and the trisomy16 mouse. *Trends Neurosci.* 1988;11:390-394.
  5. Hook EB. Issues pertaining to the impact and etiology of trisomy 21 and other aneuploidy in humans; a consideration of evolutionary implications, maternal age mechanisms, and other matters. *Prog Clin Biol Res.* 1989;311:1-27.
  6. Hodgkins PS, Prasher V, Farrar G, et al. Reduced transferrin binding in Down syndrome: a route to senile plaque formation and dementia. *Neuroreport.* 1993;5:21-24.
  7. Roth GM, Sun B, Greensite FS, Lott IT, Dietrich RB. Premature aging in persons with Down syndrome: MR findings. *AJNR Am J Neuroradiol.* 1996;17:1283-1289.
  8. Chapman RS, Hesketh LJ. Behavioral phenotype of individuals with Down syndrome. *Ment Retard Dev Disabil Res Rev.* 2000;6:84-95.
  9. Cataldo AM, Peterhoff CM, Troncoso JC, Gomez-Isla T, Hyman BT, Nixon RA. Endocytic pathway abnormalities precede amyloid beta deposition in sporadic Alzheimer's disease and Down syndrome: differential effects of APOE genotype and presenilin mutations. *Am J Pathol.* 2000;157:277-286.
  10. Hartley D, Blumenthal T, Carrillo M, et al. Down syndrome and Alzheimer's disease: common pathways, common goals. *Alzheimers Dement.* 2015;11:700-709.
  11. Hartley SL, Handen BL, Devenny DA, et al. Cognitive functioning in relation to brain amyloid-beta in healthy adults with Down syndrome. *Brain.* 2014;137:2556-2563.
  12. Leverenz JB, Raskind MA. Early amyloid deposition in the medial temporal lobe of young Down syndrome patients: a regional quantitative analysis. *Exp Neurol.* 1998;150:296-304.
  13. Wisniewski KE, Dalton AJ, Crapper McLachlan DR, Wen GY, Wisniewski HM. Alzheimer's disease in Down's syndrome: clinicopathologic studies. *Neurology.* 1985;35:957-961.
  14. Lai F, Williams RS. A prospective study of Alzheimer disease in Down syndrome. *Arch Neurol.* 1989;46:849-853.
  15. Perez SE, Miguel JC, He B, et al. Frontal cortex and striatal cellular and molecular pathobiology in individuals with Down syndrome with and without dementia. *Acta Neuropathol.* 2019;137:413-436.
  16. Videla L, Benejam B, Pegueroles J, et al. Longitudinal clinical and cognitive changes along the Alzheimer disease continuum in Down syndrome. *JAMA Netw Open.* 2022;5:e2225573.
  17. Hill DA, Gridley G, Cnattingius S, et al. Mortality and cancer incidence among individuals with Down syndrome. *Arch Intern Med.* 2003;163:705-711.
  18. Bittles AH, Bower C, Hussain R, Glasson EJ. The four ages of Down syndrome. *Eur J Public Health.* 2007;17:221-225.
  19. Presson AP, Partyka G, Jensen KM, et al. Current estimate of Down syndrome population prevalence in the United States. *J Pediatr.* 2013;163:1163-1168.
  20. Dick MB, Doran E, Phelan M, Lott IT. Cognitive profiles on the severe impairment battery are similar in Alzheimer Disease and Down Syndrome with Dementia. *Alzheimer Dis Assoc Disord.* 2016;30(3):251-257. doi:10.1097/WAD.000000000000132. PMID: 26704220; PMCID: PMC5860802.
  21. Hithersay R, Startin CM, Hamburg S, et al. Association of dementia with mortality among adults with Down syndrome older than 35 years. *JAMA Neurol.* 2019;76:152-160.
  22. Sendera TJ, Ma SY, Jaffar S, et al. Reduction in TrkA-immunoreactive neurons is not associated with an overexpression of galaninergic fibers within the nucleus basalis in Down's syndrome. *J Neurochem.* 2000;74:1185-1196.
  23. Mufson EJ, Bothwell M, Kordower JH. Loss of nerve growth factor receptor-containing neurons in Alzheimer's disease: a quantitative analysis across subregions of the basal forebrain. *Exp Neurol.* 1989;105:221-232.
  24. Mann DM, Yates PO, Marcyniuk B, Ravindra CR. The topography of plaques and tangles in Down's syndrome patients of different ages. *Neuropathol App Neurobiol.* 1986;12:447-457.
  25. Wegiel J, Flory M, Kuchna I, et al. Developmental deficits and staging of dynamics of age associated Alzheimer's disease neurodegeneration and neuronal loss in subjects with Down syndrome. *Acta Neuropathol Commun.* 2022;10:2.
  26. Richter N, David LS, Grothe MJ, et al. Age and anterior basal forebrain volume predict the cholinergic deficit in patients with mild cognitive impairment due to Alzheimer's disease. *J Alzheimers Dis.* 2022;86:425-440.
  27. Belichenko PV, Kleschevnikov AM, Masliah E, et al. Excitatory-inhibitory relationship in the fascia dentata in the Ts65Dn mouse model of Down syndrome. *J Comp Neurol.* 2009;512:453-466.
  28. Belichenko PV, Masliah E, Kleschevnikov AM, et al. Synaptic structural abnormalities in the Ts65Dn mouse model of Down syndrome. *J Comp Neurol.* 2004;480:281-298.
  29. Granholm AC, Sanders LA, Crnic LS. Loss of cholinergic phenotype in basal forebrain coincides with cognitive decline in a mouse model of Down's syndrome. *Exp Neurol.* 2000;161:647-663.
  30. Kelley CM, Powers BE, Velazquez R, et al. Sex differences in the cholinergic basal forebrain in the Ts65Dn mouse model of Down syndrome and Alzheimer's disease. *Brain Pathol.* 2014;24:33-44.
  31. Kelley CM, Powers BE, Velazquez R, et al. Maternal choline supplementation differentially alters the basal forebrain cholinergic system of young-adult Ts65Dn and disomic mice. *J Comp Neurol.* 2014;522:1390-1410.
  32. Cooper JD, Salehi A, Delcroix JD, et al. Failed retrograde transport of NGF in a mouse model of Down's syndrome: reversal of cholinergic neurodegenerative phenotypes following NGF infusion. *Proc Natl Acad Sci USA.* 2001;98:10439-10444.
  33. Sans-Dublanc A, Razzauti A, Desikan S, Pascual M, Monyer H, Sindreu C. Septal GABAergic inputs to CA1 govern contextual memory retrieval. *Sci Adv.* 2020;6(44):eaba5003. doi:10.1126/sciadv.aba5003. PMID: 33127668; PMCID: PMC7608800.
  34. Fernandez F, Morishita W, Zuniga E, et al. Pharmacotherapy for cognitive impairment in a mouse model of Down syndrome. *Nat Neurosci.* 2007;10:411-413.
  35. Contestabile A, Magara S, Cancedda L. The GABAergic hypothesis for cognitive disabilities in Down syndrome. *Front Cell Neurosci.* 2017;11:54.

36. Givens BS, Olton DS. Cholinergic and GABAergic modulation of medial septal area: effect on working memory. *Behav Neurosci.* 1990;104:849-855.
37. Mesulam MM, Mufson EJ, Wainer BH, Levey AI. Central cholinergic pathways in the rat: an overview based on an alternative nomenclature (Ch1-Ch6). *Neuroscience.* 1983;10:1185-1201.
38. Lockrow J, Prakasam A, Huang P, Bimonte-Nelson H, Sambamurti K, Granholm AC. Cholinergic degeneration and memory loss delayed by vitamin E in a Down syndrome mouse model. *Exp Neurol.* 2009;216:278-289.
39. Hunter CL, Bimonte-Nelson HA, Nelson M, Eckman CB, Granholm AC. Behavioral and neurobiological markers of Alzheimer's disease in Ts65Dn mice: effects of estrogen. *Neurobiol Aging.* 2004;25:873-884.
40. Holtzman DM, Santucci D, Kilbridge J, et al. Developmental abnormalities and age-related neurodegeneration in a mouse model of Down syndrome. *Proc Natl Acad Sci U S A.* 1996;93:13333-13338.
41. Powers BE, Kelley CM, Velazquez R, et al. Maternal choline supplementation in a mouse model of Down syndrome: effects on attention and nucleus basalis/substantia innominata neuron morphology in adult offspring. *Neuroscience.* 2017;340:501-514.
42. Powers BE, Velazquez R, Kelley CM, et al. Attentional function and basal forebrain cholinergic neuron morphology during aging in the Ts65Dn mouse model of Down syndrome. *Brain Struct Funct.* 2016;221:4337-4352.
43. Ash JA, Velazquez R, Kelley CM, et al. Maternal choline supplementation improves spatial mapping and increases basal forebrain cholinergic neuron number and size in aged Ts65Dn mice. *Neurobiol Dis.* 2014;70:32-42.
44. Kelley CM, Ash JA, Powers BE, et al. Effects of maternal choline supplementation on the septohippocampal cholinergic system in the Ts65Dn mouse model of Down syndrome. *Curr Alzheimer Res.* 2016;13:84-96.
45. Strupp BJ, Powers BE, Velazquez R, et al. Maternal choline supplementation: a potential prenatal treatment for Down syndrome and Alzheimer's disease. *Curr Alzheimer Res.* 2016;13:97-106.
46. Moon J, Chen M, Gandhi SU, et al. Perinatal choline supplementation improves cognitive functioning and emotion regulation in the Ts65Dn mouse model of Down syndrome. *Behav Neurosci.* 2010;124:346-361.
47. Hunter CL, Bimonte HA, Granholm A-CE. Behavioral comparison of 4 and 6 month-old Ts65Dn mice: age-related impairments in working and reference memory. *Behav Brain Res.* 2003;138:121-131.
48. Kelley CM, Ginsberg SD, Alldred MJ, Strupp BJ, Mufson EJ. Maternal choline supplementation alters basal forebrain cholinergic neuron gene expression in the Ts65Dn mouse model of Down syndrome. *Dev Neurobiol.* 2019;79:664-683.
49. Cataldo AM, Petanceska S, Peterhoff CM, et al. App gene dosage modulates endosomal abnormalities of Alzheimer's disease in a segmental trisomy 16 mouse model of Down syndrome. *J Neurosci.* 2003;23:6788-6792.
50. Hunter CL, Isacson O, Nelson M, et al. Regional alterations in amyloid precursor protein and nerve growth factor across age in a mouse model of Down's syndrome. *Neurosci Res.* 2003;45:437-445.
51. Contestabile A, Fila T, Bartesaghi R, Ciani E. Choline acetyltransferase activity at different ages in brain of Ts65Dn mice, an animal model for Down's syndrome and related neurodegenerative diseases. *J Neurochem.* 2006;97:515-526.
52. Alldred MJ, Penikalapati SC, Lee SH, Heguy A, Roussos P, Ginsberg SD. Profiling basal forebrain cholinergic neurons reveals a molecular basis for vulnerability within the Ts65Dn model of Down syndrome and Alzheimer's disease. *Mol Neurobiol.* 2021;58:5141-5162.
53. Davenport C, Yan J, Taesuwan S, et al. Choline intakes exceeding recommendations during human lactation improve breast milk choline content by increasing PEMT pathway metabolites. *J Nutr Biochem.* 2015;26:903-911.
54. Ganz AB, Cohen VV, Swersky CC, et al. Genetic variation in choline-metabolizing enzymes alters choline metabolism in young women consuming choline intakes meeting current recommendations. *Int J Mol Sci.* 2017;18(2):252. doi:10.3390/ijms18020252. PMID: 28134761; PMCID: PMC5343788.
55. Caudill MA, Strupp BJ, Muscalu L, Nevins JEH, Canfield RL. Maternal choline supplementation during the third trimester of pregnancy improves infant information processing speed: a randomized, double-blind, controlled feeding study. *FASEB J.* 2018;32:2172-2180.
56. Zeisel SH. Nutrition in pregnancy: the argument for including a source of choline. *Int J Womens Health.* 2013;5:193-199.
57. Gwee MC, Sim MK. Free choline concentration and cephalin-N-methyltransferase activity in the maternal and foetal liver and placenta of pregnant rats. *Clin Exp Pharmacol Physiol.* 1978;5:649-653.
58. Institute of Medicine, N. A. o. S. U. *Dietary Reference Intakes for Thiamin, Riboflavin, Niacin, Vitamin B6, Folate, Vitamin B12, Pantothenic Acid, Biotin and Choline.* National Academy Press; 1998.
59. Meck WH, Smith RA, Williams CL. Organizational changes in cholinergic activity and enhanced visuospatial memory as a function of choline administered prenatally or postnatally or both. *Behav Neurosci.* 1989;103:1234-1241.
60. Zeisel SH, Klatt KC, Caudill MA. Choline. *Adv Nutr.* 2018;9:58-60.
61. Blusztajn JK. Choline, a vital amine. *Science.* 1998;281:794-795.
62. Blusztajn JK, Mellott TJ. Neuroprotective actions of perinatal choline nutrition. *Clin Chem Lab Med.* 2013;51:591-599.
63. McGowan PO, Meaney MJ, Szyf M. Diet and the epigenetic (re) programming of phenotypic differences in behavior. *Brain Res.* 2008;1237:12-24.
64. Kwan STC, King JH, Grenier JK, et al. Maternal choline supplementation during normal murine pregnancy alters the placental epigenome: results of an exploratory study. *Nutrients.* 2018;10(4):417. doi:10.3390/nu10040417. PMID: 29597262; PMCID: PMC5946202.
65. Blusztajn JK, Slack BE, Mellott TJ. Neuroprotective actions of dietary choline. *Nutrients.* 2017;9(8):815. doi:10.3390/nu9080815. PMID: 28788094; PMCID: PMC5579609.
66. Yan J, Ginsberg SD, Powers B, et al. Maternal choline supplementation programs greater activity of the phosphatidylethanolamine N-methyltransferase (PEMT) pathway in adult Ts65Dn trisomic mice. *FASEB J.* 2014;28:4312-4323.
67. Meck WH, Smith RA, Williams CL. Pre- and postnatal choline supplementation produces long-term facilitation of spatial memory. *Dev Psychobiol.* 1988;21:339-353.

68. Jiang X, Yan J, West AA, et al. Maternal choline intake alters the epigenetic state of fetal cortisol-regulating genes in humans. *FASEB J*. 2012;26:3563-3574.
69. Korsmo HW, Jiang X, Caudill MA. Choline: exploring the growing science on its benefits for moms and babies. *Nutrients*. 2019;11(8):1823. doi:10.3390/nu11081823. PMID: 31394787; PMCID: PMC6722688.
70. Powers BE, Velazquez R, Strawderman MS, Ginsberg SD, Mufson EJ, Strupp BJ. Maternal choline supplementation as a potential therapy for Down syndrome: assessment of effects throughout the lifespan. *Front Aging Neurosci*. 2021;13:723046.
71. Taesuwan S, McDougall MQ, Malysheva OV, et al. Choline metabolome response to prenatal choline supplementation across pregnancy: a randomized controlled trial. *FASEB J*. 2021;35:e22063.
72. Warton FL, Molteno CD, Warton CMR, et al. Maternal choline supplementation mitigates alcohol exposure effects on neonatal brain volumes. *Alcohol Clin Exp Res*. 2021;45:1762-1774.
73. Velazquez R, Ferreira E, Knowles S, et al. Lifelong choline supplementation ameliorates Alzheimer's disease pathology and associated cognitive deficits by attenuating microglia activation. *Aging Cell*. 2019;18:e13037.
74. Velazquez R, Ash JA, Powers BE, et al. Maternal choline supplementation improves spatial learning and adult hippocampal neurogenesis in the Ts65Dn mouse model of Down syndrome. *Neurobiol Dis*. 2013;58:92-101.
75. Alldred MJ, Chao HM, Lee SH, et al. CA1 pyramidal neuron gene expression mosaics in the Ts65Dn murine model of Down syndrome and Alzheimer's disease following maternal choline supplementation. *Hippocampus*. 2018;28:251-268.
76. Alldred MJ, Chao HM, Lee SH, et al. Long-term effects of maternal choline supplementation on CA1 pyramidal neuron gene expression in the Ts65Dn mouse model of Down syndrome and Alzheimer's disease. *FASEB J*. 2019;33:9871-9884.
77. Bahnfleth CL, Strupp BJ, Caudill MA, Canfield RL. Prenatal choline supplementation improves child sustained attention: a 7-year follow-up of a randomized controlled feeding trial. *FASEB J*. 2022;36:e22054.
78. Alldred MJ, Lee SH, Petkova E, Ginsberg SD. Expression profile analysis of hippocampal CA1 pyramidal neurons in aged Ts65Dn mice, a model of Down syndrome (DS) and Alzheimer's disease (AD). *Brain Struct Funct*. 2015b;220:2983-2996.
79. Alldred MJ, Lee SH, Petkova E, Ginsberg SD. Expression profile analysis of vulnerable CA1 pyramidal neurons in young-middle-aged Ts65Dn mice. *J Comp Neurol*. 2015a;523:61-74.
80. Detopoulou P, Panagiotakos DB, Antonopoulou S, Pitsavos C, Stefanadis C. Dietary choline and betaine intakes in relation to concentrations of inflammatory markers in healthy adults: the ATTICA study. *Am J Clin Nutr*. 2008;87:424-430.
81. Duchon A, Raveau M, Chevalier C, Nalesso V, Sharp AJ, Herault Y. Identification of the translocation breakpoints in the Ts65Dn and Ts1Cje mouse lines: relevance for modeling Down syndrome. *Mamm Genome*. 2011;22:674-684.
82. Andrews S. FastQC: a quality control tool for high throughput sequence data. 2010 [Online]. Accessed May 8, 2023. <http://www.bioinformatics.babraham.ac.uk/projects/fastqc/>
83. Bolger AM, Lohse M, Usadel B. Trimmomatic: a flexible trimmer for Illumina sequence data. *Bioinformatics (Oxford, England)*. 2014;30:2114-2120.
84. Dobin A, Davis CA, Schlesinger F, et al. STAR: ultrafast universal RNA-seq aligner. *Bioinformatics (Oxford, England)*. 2013;29:15-21.
85. Picard Toolkit. *Broad Institute, GitHub Repository*. Broad Institute; 2019. Accessed May 8, 2023. <https://broadinstitute.github.io/picard/>
86. Li B, Dewey CN. RSEM: accurate transcript quantification from RNA-seq data with or without a reference genome. *BMC Bioinform*. 2011;12:323.
87. Wang L, Wang S, Li W. RSeQC: quality control of RNA-seq experiments. *Bioinformatics (Oxford, England)*. 2012;28:2184-2185.
88. Robinson MD, Oshlack A. A scaling normalization method for differential expression analysis of RNA-seq data. *Genome Biol* 11, R25 (2010). <https://doi.org/10.1186/gb-2010-11-3-r25>
89. Robinson MD, McCarthy DJ, Smyth GK. edgeR: a Bioconductor package for differential expression analysis of digital gene expression data. *Bioinformatics (Oxford, England)*. 2010;26:139-140.
90. Zehetmayer S, Posch M, Graf A. Impact of adaptive filtering on power and false discovery rate in RNA-seq experiments. *BMC Bioinform*. 2022;23:388.
91. Rau A, Gallopin M, Celeux G, Jaffrézic F. Data-based filtering for replicated high-throughput transcriptome sequencing experiments. *Bioinformatics (Oxford, England)*. 2013;29:2146-2152.
92. Hoffman GE, Roussos P. Dream: powerful differential expression analysis for repeated measures designs. *Bioinformatics (Oxford, England)*. 2021;37:192-201.
93. Hoffman GE, Schadt EE. variancePartition: interpreting drivers of variation in complex gene expression studies. *BMC Bioinform*. 2016;17:483.
94. Pagès H, Carlson M, Falcon S, Li N. AnnotationDbi: manipulation of SQLite-based annotations in Bioconductor. 2023. R package version 1.62.0. Accessed November 15, 2021. <https://bioconductor.org/packages/AnnotationDbi>
95. Broberg P. A comparative review of estimates of the proportion unchanged genes and the false discovery rate. *BMC Bioinformatics*. 2005;6:199.
96. QIAGEN IPA. (2020) QIAGEN Inc. Accessed May 8, 2021. <https://digitalinsights.qiagen.com/IPA>
97. Krämer A, Green J, Pollard J Jr, Tugendreich S. Causal analysis approaches in ingenuity pathway analysis. *Bioinformatics (Oxford, England)*. 2013;30:523-530.
98. Kanehisa M, Goto S. KEGG: Kyoto encyclopedia of genes and genomes. *Nucleic Acids Res*. 2000;28:27-30.
99. Ashburner M, Ball CA, Blake JA, et al. Gene ontology: tool for the unification of biology. The gene ontology consortium. *Nat Genet*. 2000;25:25-29.
100. The gene ontology resource: enriching a Gold mine. *Nucl Acids Res*. 2021;49:D325-D334.
101. Szklarczyk D, Gable AL, Lyon D, et al. STRING v11: protein-protein association networks with increased coverage, supporting functional discovery in genome-wide experimental datasets. *Nucleic Acids Res*. 2018;47:D607-D613.
102. Shannon P, Markiel A, Ozier O, et al. Cytoscape: a software environment for integrated models of biomolecular interaction networks. *Genome Res*. 2003;13:2498-2504.
103. Ginsberg SD, Che S. Combined histochemical staining, RNA amplification, regional, and single cell cDNA analysis within the hippocampus. *Lab Invest*. 2004;84:952-962.

104. Alldred MJ, Lee SH, Ginsberg SD. Adiponectin modulation by genotype and maternal choline supplementation in a mouse model of Down Syndrome and Alzheimer's Disease. *J Clin Med*. 2021;10(13):2994. doi:10.3390/jcm10132994. PMID: 34279477; PMCID: PMC8267749.
105. Alldred MJ, Lee SH, Stutzmann GE, Ginsberg SD. Oxidative phosphorylation is dysregulated within the basocortical circuit in a 6-month old mouse model of Down syndrome and Alzheimer's disease. *Front Aging Neurosci*. 2021;13:707950.
106. Ginsberg SD, Alldred MJ, Counts SE, et al. Microarray analysis of hippocampal CA1 neurons implicates early endosomal dysfunction during Alzheimer's disease progression. *Biol Psychiatry*. 2010;68:885-893.
107. Jiang Y, Mullaney KA, Peterhoff CM, et al. Alzheimer's-related endosome dysfunction in Down syndrome is Abeta-independent but requires APP and is reversed by BACE-1 inhibition. *Proc Natl Acad Sci USA*. 2010;107:1630-1635.
108. ABI. Guide to performing relative quantitation of gene expression using real-time quantitative PCR. *Appl Biosyst Product Guide*. 2004;1:1-60.
109. Chen Y, Dyakin VV, Branch CA, et al. In vivo MRI identifies cholinergic circuitry deficits in a Down syndrome model. *Neurobiol Aging*. 2009;30:1453-1465.
110. Dai G, Yu H, Kruse M, Traynor-Kaplan A, Hille B. Osmoregulatory inositol transporter SMIT1 modulates electrical activity by adjusting PI(4,5)P2 levels. *Proc Natl Acad Sci USA*. 2016;113:E3290-E3299.
111. Grosse G, Draguhn A, Höhne L, Tapp R, Veh RW, Ahnert-Hilger G. Expression of Kv1 potassium channels in mouse hippocampal primary cultures: development and activity-dependent regulation. *J Neurosci*. 2000;20:1869-1882.
112. Liu F, Liang Z, Wegiel J, et al. Overexpression of Dyrk1A contributes to neurofibrillary degeneration in Down syndrome. *FASEB J*. 2008;22:3224-3233.
113. Ferrer I, Barrachina M, Puig B, et al. Constitutive Dyrk1A is abnormally expressed in Alzheimer disease, Down syndrome, Pick disease, and related transgenic models. *Neurobiol Dis*. 2005;20:392-400.
114. Zarouchlioti C, Parfitt DA, Li W, Gittings LM, Cheetham ME. DNAP proteins in neurodegeneration: essential and protective factors. *Philos Trans R Soc Lond B Biol Sci*. 2018;373:20160534.
115. Fulton SL, Wenderski W, Lepack AE, et al. Rescue of deficits by Brwd1 copy number restoration in the Ts65Dn mouse model of Down syndrome. *Nat Commun*. 2022;13:6384.
116. Wolvetang EJ, Bradfield OM, Hatzistavrou T, et al. Overexpression of the chromosome 21 transcription factor Ets2 induces neuronal apoptosis. *Neurobiol Dis*. 2003;14:349-356.
117. Yu Y, Chu PY, Bowser DN, et al. Mice deficient for the chromosome 21 ortholog Itsn1 exhibit vesicle-trafficking abnormalities. *Hum Mol Genet*. 2008;17:3281-3290.
118. Schliebs R, Arendt T. The cholinergic system in aging and neuronal degeneration. *Behav Brain Res*. 2011;221:555-563.
119. Perry EK, Perry RH, Smith CJ, et al. Cholinergic receptors in cognitive disorders. *Can J Neurol Sci*. 1986;13:521-527.
120. Kolisnyk B, Al-Onaizi M, Soreq L, et al. Cholinergic surveillance over hippocampal RNA metabolism and Alzheimer's-like pathology. *Cereb Cortex*. 2017;27:3553-3567.
121. Ferreira-Vieira TH, Guimaraes IM, Silva FR, Ribeiro FM. Alzheimer's disease: targeting the cholinergic system. *Curr Neuropharmacol*. 2016;14:101-115.
122. Kurimoto E, Yamada R, Hirakawa T, Kimura H. Therapeutic potential of TAK-071, a muscarinic M(1) receptor positive allosteric modulator with low cooperativity, for the treatment of cognitive deficits and negative symptoms associated with schizophrenia. *Neurosci Lett*. 2021;764:136240.
123. Sabbir MG, Speth RC, Albensi BC. Loss of cholinergic receptor muscarinic 1 (CHRM1) protein in the hippocampus and temporal cortex of a subset of individuals with Alzheimer's disease, Parkinson's disease, or frontotemporal dementia: implications for patient survival. *J Alzheimers Dis*. 2022;90:727-747.
124. Liu W, Li J, Yang M, et al. Chemical genetic activation of the cholinergic basal forebrain hippocampal circuit rescues memory loss in Alzheimer's disease. *Alzheimers Res Ther*. 2022;14:53.
125. Kaur G, Sharma A, Xu W, et al. Glutamatergic transmission aberration: a major cause of behavioral deficits in a murine model of Down's syndrome. *J Neurosci*. 2014;34:5099-5106.
126. Rueda N, Llorens-Martin M, Florez J, et al. Memantine normalizes several phenotypic features in the Ts65Dn mouse model of Down syndrome. *J Alzheimers Dis*. 2010;21:277-290.
127. Lockrow J, Boger H, Bimonte-Nelson H, Granholm AC. Effects of long-term memantine on memory and neuropathology in Ts65Dn mice, a model for Down syndrome. *Behav Brain Res*. 2011;221:610-622.
128. Dave N, Judd JM, Decker A, et al. Dietary choline intake is necessary to prevent systems-wide organ pathology and reduce Alzheimer's disease hallmarks. *Aging Cell*. 2023;22:e13775.
129. Paoletti P, Bellone C, Zhou Q. NMDA receptor subunit diversity: impact on receptor properties, synaptic plasticity and disease. *Nat Rev Neurosci*. 2013;14:383-400.
130. Babaei P. NMDA and AMPA receptors dysregulation in Alzheimer's disease. *Eur J Pharmacol*. 2021;908:174310.
131. Ginsberg SD, Hemby SE, Lee VM, Eberwine JH, Trojanowski JQ. Expression profile of transcripts in Alzheimer's disease tangle-bearing CA1 neurons. *Ann Neurol*. 2000;48:77-87.
132. Conejero-Goldberg C, Hyde TM, Chen S, et al. Molecular signatures in post-mortem brain tissue of younger individuals at high risk for Alzheimer's disease as based on APOE genotype. *Mol Psychiatry*. 2011;16:836-847.
133. Moretto E, Murru L, Martano G, Sassone J, Passafaro M. Glutamatergic synapses in neurodevelopmental disorders. *Progr Neuro-Psychopharmacol Biol Psych*. 2018;84:328-342.
134. Schwenk J, Baehrens D, Haupt A, et al. Regional diversity and developmental dynamics of the AMPA-receptor proteome in the mammalian brain. *Neuron*. 2014;84:41-54.
135. Oka A, Takashima S. The up-regulation of metabotropic glutamate receptor 5 (mGluR5) in Down's syndrome brains. *Acta Neuropathol*. 1999;97:275-278.
136. Dölen G, Osterweil E, Rao BS, et al. Correction of fragile X syndrome in mice. *Neuron*. 2007;56:955-962.
137. Rudolph U, Mohler H. GABAA receptor subtypes: therapeutic potential in Down syndrome, affective disorders, schizophrenia, and autism. *Annu Rev Pharmacol Toxicol*. 2014;54:483-507.
138. Milenkovic I, Stojanovic T, Aronica E, et al. GABA(a) receptor subunit deregulation in the hippocampus of human fetuses with Down syndrome. *Brain Struct Funct*. 2018;223:1501-1518.
139. Rueda N, Florez J, Martinez-Cue C. Mouse models of Down syndrome as a tool to unravel the causes of mental disabilities. *Neural Plast*. 2012;2012:584071.

140. Rueda N, Flórez J, Dierssen M, Martínez-Cué C. Translational validity and implications of pharmacotherapies in preclinical models of Down syndrome. *Prog Brain Res.* 2020;251:245-268.
141. Miller LG, Greenblatt DJ, Roy RB, Lopez F, Wecker L. Dietary choline intake modulates benzodiazepine receptor binding and gamma-aminobutyric acidA receptor function in mouse brain. *J Pharmacol Exp Ther.* 1989;248:1-6.
142. Schweizer C, Balsiger S, Bluethmann H, et al. The gamma 2 subunit of GABA(a) receptors is required for maintenance of receptors at mature synapses. *Mol Cell Neurosci.* 2003;24:442-450.
143. Lorenz-Guertin JM, Bambino MJ, Jacob TC.  $\gamma$ 2 GABA(a)R trafficking and the consequences of human genetic variation. *Front Cell Neurosci.* 2018;12:265.
144. Tyagarajan SK, Fritschy JM. GABA(a) receptors, gephyrin and homeostatic synaptic plasticity. *J Physiol.* 2010;588:101-106.
145. Brickley SG, Mody I. Extrasynaptic GABA(A) receptors: their function in the CNS and implications for disease. *Neuron.* 2012;73:23-34.
146. Das D, Phillips C, Hsieh W, Sumanth K, Dang V, Salehi A. Neurotransmitter-based strategies for the treatment of cognitive dysfunction in Down syndrome. *Prog Neuropsychopharmacol Biol Psychiatry.* 2014;54:140-148.
147. Belichenko PV, Kleschevnikov AM, Salehi A, Epstein CJ, Mobley WC. Synaptic and cognitive abnormalities in mouse models of Down syndrome: exploring genotype-phenotype relationships. *J Comp Neurol.* 2007;504:329-345.
148. Carbonell J, Blasco-Ibáñez JM, Crespo C, Náchter J, Varea E. Piriform cortex alterations in the Ts65Dn model for Down syndrome. *Brain Res.* 2020;1747:147031.
149. Zeisel SH. Choline: clinical nutrigenetic/nutrigenomic approaches for identification of functions and dietary requirements. *J Nutrigenet Nutrigenomics.* 2010;3:209-219.
150. Cirillo E, Parnell LD, Evelo CT. A review of pathway-based analysis tools that visualize genetic variants. *Front Genet.* 2017;8:174.
151. Choong XY, Tosh JL, Pulford LJ, Fisher EM. Dissecting Alzheimer disease in Down syndrome using mouse models. *Front Behav Neurosci.* 2015;9:268.
152. Gupta M, Dhanasekaran AR, Gardiner KJ. Mouse models of Down syndrome: gene content and consequences. *Mamm Genome.* 2016;27:538-555.
153. Gardiner K, Fortna A, Bechtel L, Davisson MT. Mouse models of Down syndrome: how useful can they be? Comparison of the gene content of human chromosome 21 with orthologous mouse genomic regions. *Gene.* 2003;318:137-147.
154. Sturgeon X, Gardiner KJ. Transcript catalogs of human chromosome 21 and orthologous chimpanzee and mouse regions. *Mamm Genome.* 2011;22:261-271.
155. Freund TF, Antal M. GABA-containing neurons in the septum control inhibitory interneurons in the hippocampus. *Nature.* 1988;336:170-173.
156. Gulyás AI, Hájos N, Katona I, Freund TF. Interneurons are the local targets of hippocampal inhibitory cells which project to the medial septum. *Eur J Neurosci.* 2003;17:1861-1872.

### SUPPORTING INFORMATION

Additional supporting information can be found online in the Supporting Information section at the end of this article.

**How to cite this article:** Allred MJ, Pidikiti H, Heguy A, Roussos P, Ginsberg SD. Basal forebrain cholinergic neurons are vulnerable in a mouse model of Down syndrome and their molecular fingerprint is rescued by maternal choline supplementation. *The FASEB Journal.* 2023;37:e22944. doi:[10.1096/fj.202202111RR](https://doi.org/10.1096/fj.202202111RR)